‘McArthur’s Zircons, a Tale of Two Arenites’ – Provenance and Evolution of the Maiwok Sub-Group, McArthur Basin, Northern Territory

Thesis submitted in accordance with the requirements of the University of Adelaide for an Honours Degree in Geology

Todd Michael Smith

November 2016

THE UNIVERSITY of ADELAIDE

'MCARTHUR'S ZIRCONS, A TALE OF TWO ARENITES' – PROVENANCE AND EVOLUTION OF THE MAIWOK SUB-GROUP, MCARTHUR BASIN, NORTHERN TERRITORY

ABSTRACT

The Beetaloo Basin is a sub-basin of the 'greater McArthur Basin', a >180,000 km2 ca. 1800-900 Ma basin system that covers much of northern Australia and, in its Mesoproterozoic section, hosts extensive hydrocarbon reserves. The nature of the basin and provenance of the rocks within the basin is largely unknown.
Here I present detrital zircon U-Pb data from twelve sandstone core samples from the Maiwok Sub-group, and compare with existing outcrop samples from the Urapunga Region within the McArthur Basin to examine the maximum depositional ages of the formations, to address intra-basin correlation, and examine both temporal and spatial provenance variations. Detritus analysed yielded early Palaeoarchean to early Neoproterozoic ages from sandstone formations of the Maiwok Sub-group, in the Beetaloo Basin (Fig. 1).
In the Beetaloo Basin; the Bessie Creek Sandstone formation was deposited between 1386 ± 13 Ma and 1324 ± 8 Ma, and the Moroak Sandstone formation was deposited after1375 ± 15 Ma. The formation logged as the Moroak Sandstone (320.0-391.72m) in Altree 2 drillcore was logged incorrectly. Detrital zircon data has shown this sandstone/s is too young to be the Moroak Sandstone. I have reinterpreted this interval in Altree 2 as Bukalorkmi Sandstone from 359.5-391.72m and Jamison Sandstone from 320.0-359.5m (Fig. 7). In Altree 2, the Bukalorkmi Sandstone was deposited after to 1194 ± 25 Ma and the Jamison Sandstone was deposited between 959 ± 18 Ma and 513 ± 12 Ma.
Temporal provenance variations are minimal between the Bessie Creek Sandstone and the Moroak Sandstone, but much greater between the Moroak Sandstone and the Jamison/Bukalorkmi Sandstone formations. The Walton High defines a spatial provenance boundary from the north and the south (Fig. 12). This boundary affects Maiwok Sub-group sandstones, including exposed formations, which has been under appreciated in previous studies.

KEYWORDS

McArthur Basin, Beetaloo Basin, Roper Group, Maiwok Sub-group, Zircon Geochronology, Provenance.

TABLE OF CONTENTS

LIST OF FIGURES AND TABLES

INTRODUCTION

The Northern Territory is host to an enormous intracontinental Proterozoic basin, recently termed the 'greater McArthur Basin' (Close, 2016). The mechanism behind its formation is still under debate. The greater McArthur Basin is predominantly a sedimentary terrain (with minor igneous rocks) that covers the northern sector of the Northern Territory. It is so vast (Fig. 1) that it extends into Western Australia, Queensland and likely extends into the submarine Arafura Basin, off the northern Australian coastline (Rawlings, 1999; Ahmad and Munson, 2013; Munson, 2016). The greater McArthur Basin includes the sub-surface Beetaloo Basin, cropping out in the northeast of the Northern Territory, the Birrindudu Basin, the Tomkinson Province and probably the South Nicholson Basin, (Abbott and Sweet, 2000; Betts et al., 2015; Cox et al., 2016; Munson, 2016).

The greater McArthur Basin is a frontier petroleum province and is currently the world's oldest 'live' exploration petroleum play with proven Palaeoproterozoic and Mesoproterozoic petroleum sources (Jackson et al., 1986; Ghori et al., 2009; Craig et al., 2013). Correlating wells using microfossils is difficult due to the low diversity of Mesoproterozoic eukaryotes (Javaux et al., 2004). Because of this detrital zircon geochronology is used to constrain the age of sandstones in the Beetaloo Basin, assisting with correlation, and suggesting sediment pathways from the source to the depocentre.

The Roper Group is the uppermost part of the McArthur Basin and is divided into sub-groups of alternating cross-bedded sandstones and shale formations (Jackson et al., 1999; Munson, 2016). The uppermost sub-group of the Roper Group, the Maiwok Sub-

group is dominated by shales, while the underlying Collara Sub-group is dominated by sandstones (Abbott et al., 2001).

The focus of this project is the Maiwok Sub-group, of which the Velkerri Formation is arguably the most significant formation as it has been the primary target for unconventional shale hosted reservoirs since the late 2000's (Close et al., 2016). The Beetaloo Basin is ~15,000km^2 (Ahmad and Munson, 2013), and in the targeted wells of this project, the Velkerri Formation was ~820m thick on average (but its thickness is highly variable through the basin), thus it is a large potential petroleum reservoir. I have targeted the overlying Moroak Sandstone and the underlying Bessie Creek Sandstone (Figs. 3, 4, 5), as these sandstones bracket the organic carbon rich Velkerri Formation (Revie, 2016).

Due to the substantial stratigraphic thickness and the sheer size of the unexposed Beetaloo Basin, intra-basin correlations are challenging. In addition, the tectonic geography of northern Australia through the Mesoproterozoic is controversial, as continental links have changed over time (Burrett & Berry, 2000; Gibson et al., 2012; Medig et al., 2014). I have investigated the tectonic history (Fig. 2) to produce a record of the potential provenances terranes. Detrital zircon profiles will be tabulated to link these potential provenance sources to the Beetaloo Basin, which I will use to investigate the provenance evolution record of the Bessie Creek Sandstone and the Moroak Sandstone. As well as looking at whole formation detrital zircon age distributions, I will examine intra-formation variations in the provenance profiles to see whether variations between samples are due to temporal, or lateral differences. This will help ascertain whether different sandstones reflect the erosion of different source regions, or whether the basin's sediment input has remain relative stable, and possibly parochial over time

despite changes in relative sea level. And finally the maximum deposition age of the Bessie Creek Sandstone and the Moroak Sandstone will be constrained by the youngest near-concordant zircon. To get good spatial coverage as well as samples from both sandstone formations, I have collected core samples from throughout the Beetaloo Basin (covering ~300km from north to south). Detrital zircon U-Pb data were obtained via laser ablation inductively coupled plasma mass spectrometry (LA-ICP-MS). Data are then compiled to provide maximum deposition age of the formations. These can then assist in correlating core within the basin and creating a provenance evolution record that will be compared to regional orogenic events surrounding the North Australia Craton, as well as Laurentian orogenic events, which were proximal to northern Australia at the time of deposition (Burrett and Berry, 2000) and outcrop data from the Urapunga Region (Figs. 1, 2).

GEOLOGICAL SETTING

The Roper Group was described by Rawlings (1999) as the Wilton Package, redefined by Jackson et al. (2000) as the Roper Superbasin. The Roper Group overlies an unconformity that is thought to be related to the ca. 1580-1560 Ma Isan Orogeny (Jackson et al., 1999). This forms a constraint on the maximum age of deposition of the Roper Group. The Roper Group coarsens and shoals upwards in cycles, which may have developed due to fluctuation in relative sea level (Rawlings, 1999; Abbott and Sweet, 2000). The Beetaloo Basin is the unexposed depocentre of the Roper Group, which represents the thickest part and records detailed development information (Plumb and Wellman, 1987; Abbott and Sweet, 2000; Cox et al. 2016).

The focus of this project is the upper Roper Group; the Maiwok Sub-group, which is characterised by inter-layered sandstones and shales (Jackson et al., 1999; Munson,

2016). The sandstone dominated formations, from oldest to youngest, being the Bessie Creek Sandstone, the Moroak Sandstone and the Bukalorkmi Sandstone, are typically fine to medium grained quartz rich, cross-bedded and super mature to very mature. Sulphides (such as pyrite) and glauconite are common in these sandstones and indicate reduced anoxic conditions at the time of deposition (Abbott and Sweet, 2000; Munson, 2016). These sandstone dominated formations are believed to be deposited in a shallow-marine, tidal dominated, coastal sand platform setting (Abbott and Sweet 2000; Munson, 2016).

The shale dominated formations, from oldest to youngest, are the Corcoran Formation, the Velkerri Formation and the Kyalla Formation. These are typically thinly inter-bedded laminated claystone, siltstone and minor fine grained cross-bedded sandstone, (Abbott and Sweet 2000; Munson, 2016). The Velkerri Formation and the Corcoran Formation are believed to be deposited in a low energy, basinal, off shore shelf environment, and the Kyalla Formation in an inner shelf storm dominated environment (Abbott and Sweet 2000). The Velkerri Formation and Kyalla Formation are potential targets for unconventional petroleum plays (Close et al., 2016; Revie, 2016).

The Derim Derim Dolerite intruded the Urapunga Region at 1324 ± 8 Ma (Abbott et al., 2001, 2σ error). Assuming that this is the same dolerite found in drillcores Sever 1 and Walton 2, where the Velkerri Formation (overlying the Bessie Creek Sandstone) is cross cut by dolerite, 1324 ± 8 Ma can be used to constrain the minimum age of deposition.

The Roper Group is bound by many orogenies on the North Australia Craton. These include the Arnhem Province, Arunta Region, Georgetown and Coen Region, Pine Creek Province, Halls Creek Province, Mount Isa Province and Musgrave Province (Fig. 1). These are all potential provenance sources. Past reconstructions point to the

probable connection of North Australia Craton to Laurentia, now North America. There are many Mesoproterozoic reconstruction models. I have chosen the AUSWUS reconstruction (Burrett and Berry, 2000), which is based on the Grenville orogenic belts distribution and has equivalent terranes of isotopic composition and age from the South Australia Craton juxtaposed to southern Laurentia. I have slightly modified this reconstruction, by rotating the North Australia Craton by 40° with respect to the West and South Australian Craton (Li and Evans, 2011). Based on the AUSWUS reconstruction (Burrett and Berry, 2000) I have included the Mojave Province, the Mazatzal Province and the Yavapai Province (Fig. 2) as potential provenance sources (Gibson et al., 2012; Medig et al., 2014). Data collected on these provenance terranes are compare to Beetaloo Basin drillcore samples.

There are two main hypothesised tectonic settings to explain the basin type in which the Roper Group was deposited; one suggests deposition in an extension/sag basin (Betts and Giles, 2006) and the other suggests deposition in an orogenic flexure basin (Abbott and Sweet, 2000). The latter model would predict that an active source region lay adjacent to the basin. The results of this study will help determine if this model is tenable or not.

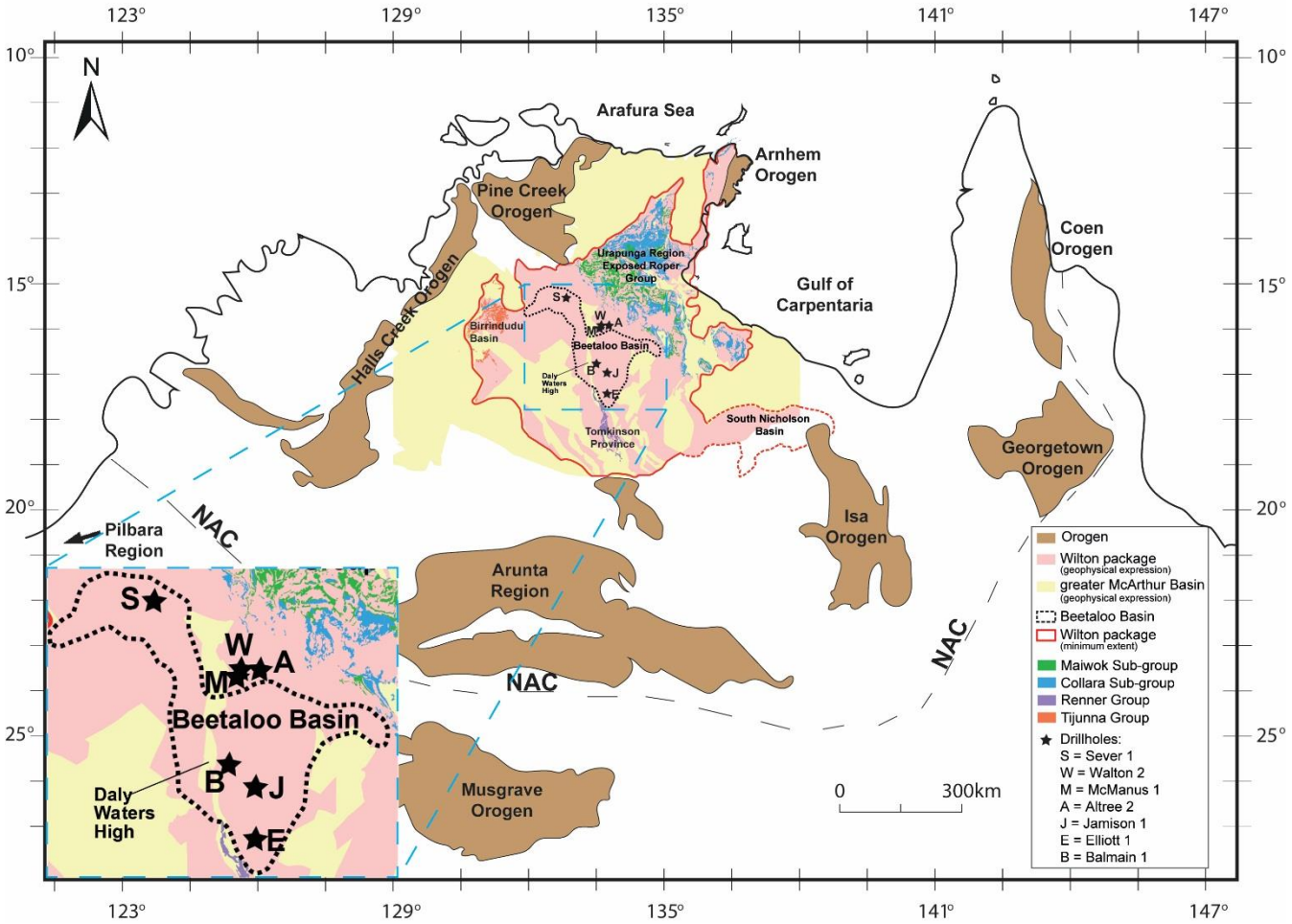

Figure 1: Locality map of the North Australian Craton (NAC), the 'greater McArthur Basin', the Beetaloo Basin, Orogenic Regions and drillholes are labelled; Sever 1, Walton 2, McManus 1, Altree 2, Jamison 1, Elliott 1, Balmain 1. (Redrafted after Betts et al., 2015; Munson, 2016).

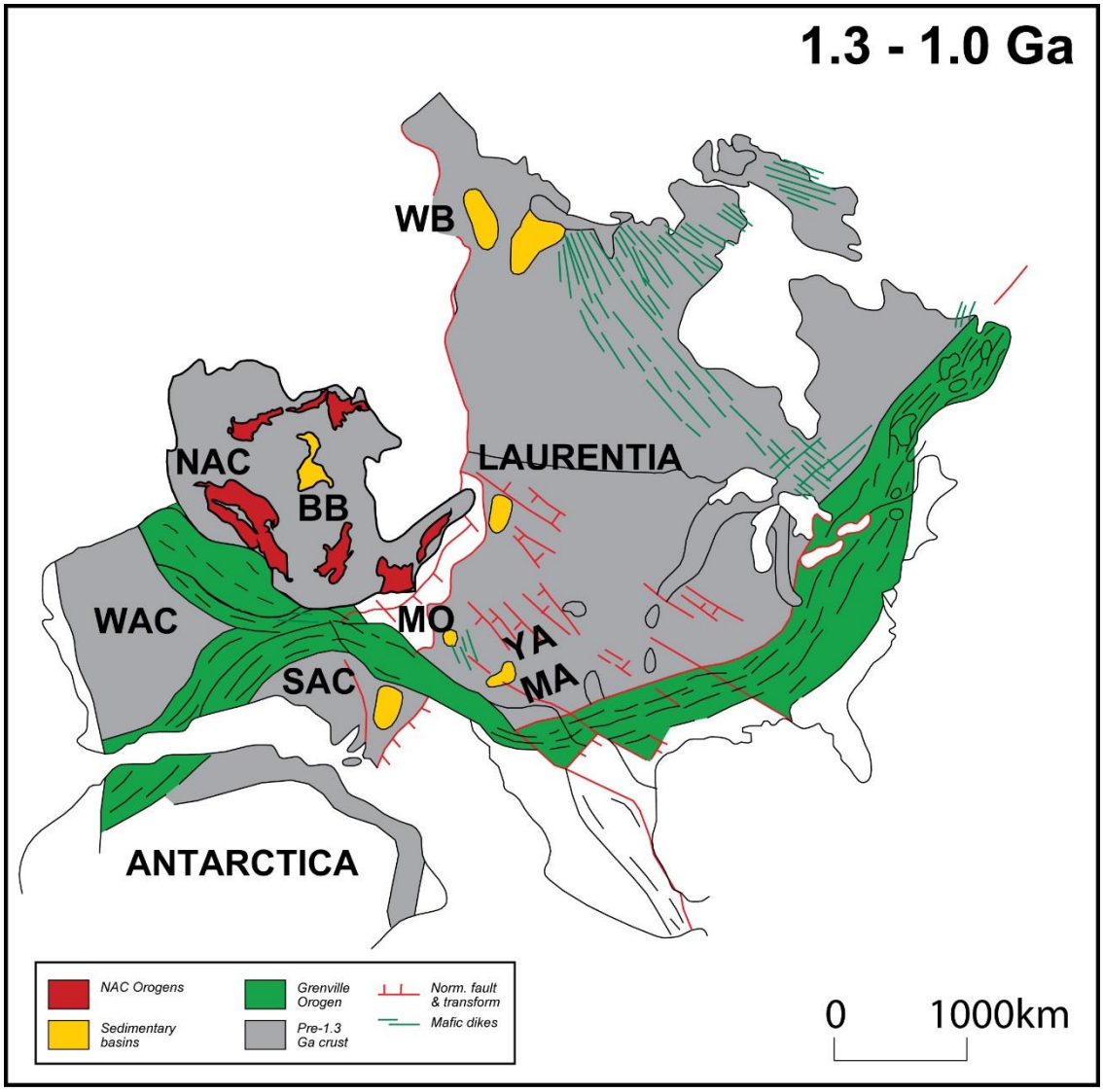

Figure 2: Modified AUSWUS reconstruction; with the North Australian Craton rotated 40º with respect to West Australian Craton (Li and Evans, 2011), the South Australian Craton juxtaposed to equivalent terranes of isotopic composition and age in southern Laurentia (Burrett & Berry, 2000), at the time of the Palaeoproterozoic Nuna supercontinent. BB = Beetaloo Basin, NAC = North Australian Craton, SAC = South Australian Craton, WAC = West Australian Craton, WB = Werneke Basin, MO = Mojave Province, YA = Yavapai Province and MA = Mazatzal Province. Modified after Burrett & Berry, 2000; Li and Evans, 2011. Note that not all sedimentary basins are displayed.

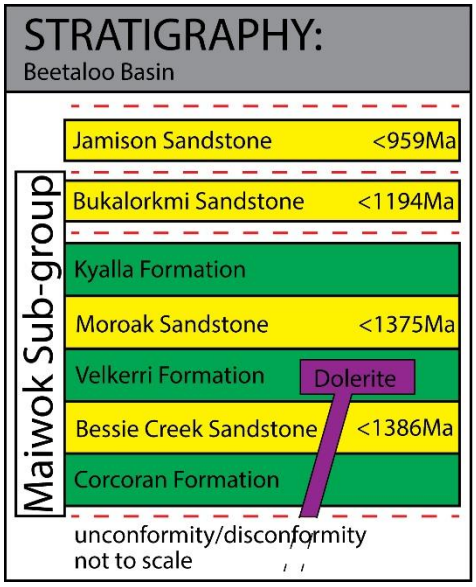

Figure 3: Simplified stratigraphy of the Maiwok Sub-group with zircon maximum depositional ages from this study labelled, in the Beetaloo Basin. Dolerite interpreted (refer to discussion) to be the equivalent age as the Derim Derim Dolerite ca. 1324 Ma (Abbott et al., 2001).

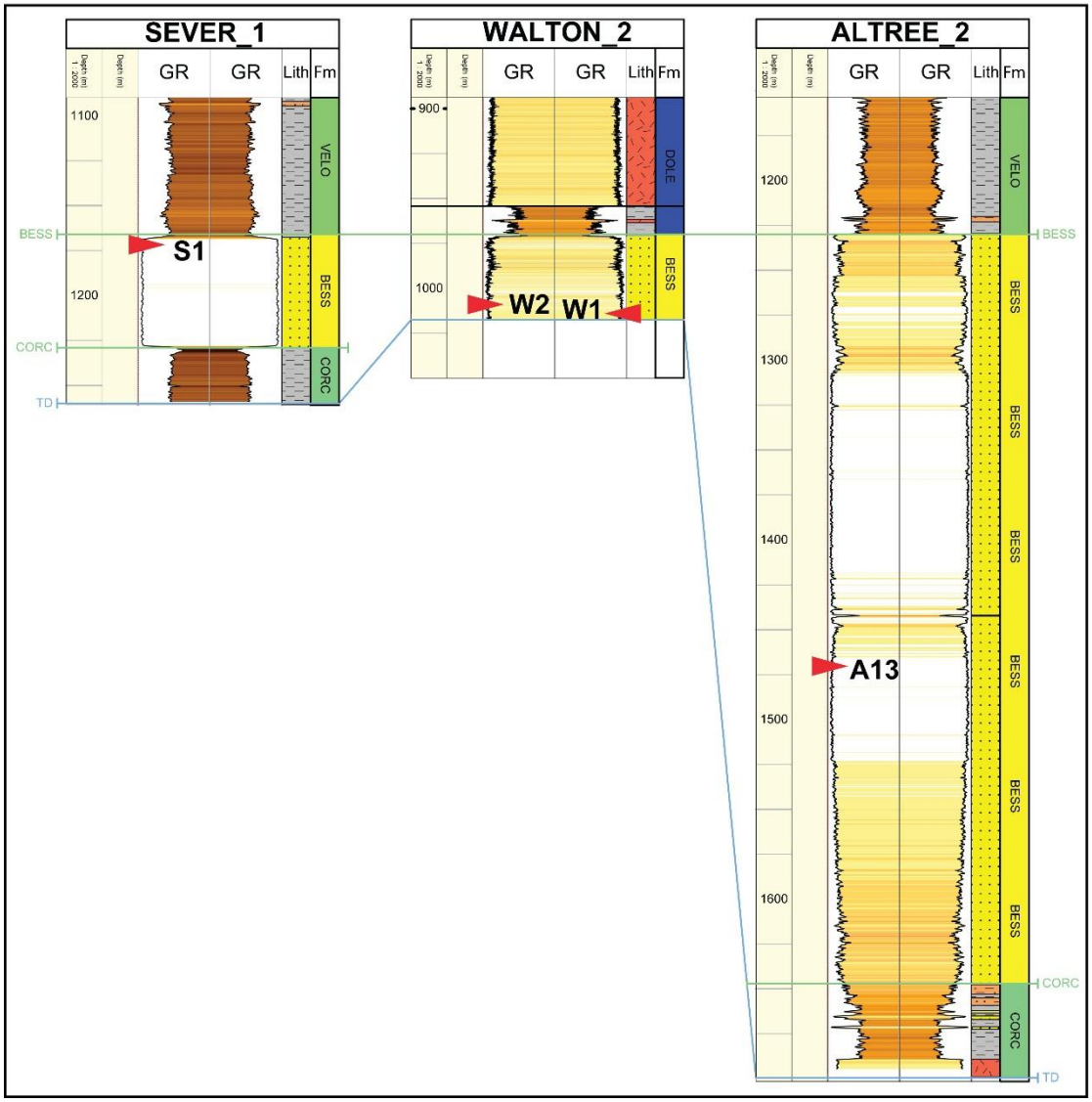

Figure 4: Vertically drilled exploration wells in the Beetaloo Basin that include the Bessie Creek Sandstone; Sever 1, Walton 2 and Altree 2 (locations in Fig.1), flattened to the top Bessie Creek Sandstone formation. GR log (mirrored), depth (m), Lith = lithology, Fm = formation, VELO = Lower Velkerri Formation, DOLE = dolerite, BESS = Bessie Creek Sandstone, CORC = Corcoran Formation, TD = Total depth of hole. Samples labelled and marked by a red arrow. Thickness of Bessie Creek Sandstone in wells: Sever 1 - 60.69m, Walton 2 - at least 49.5m, Altree 2 - 417.46m.

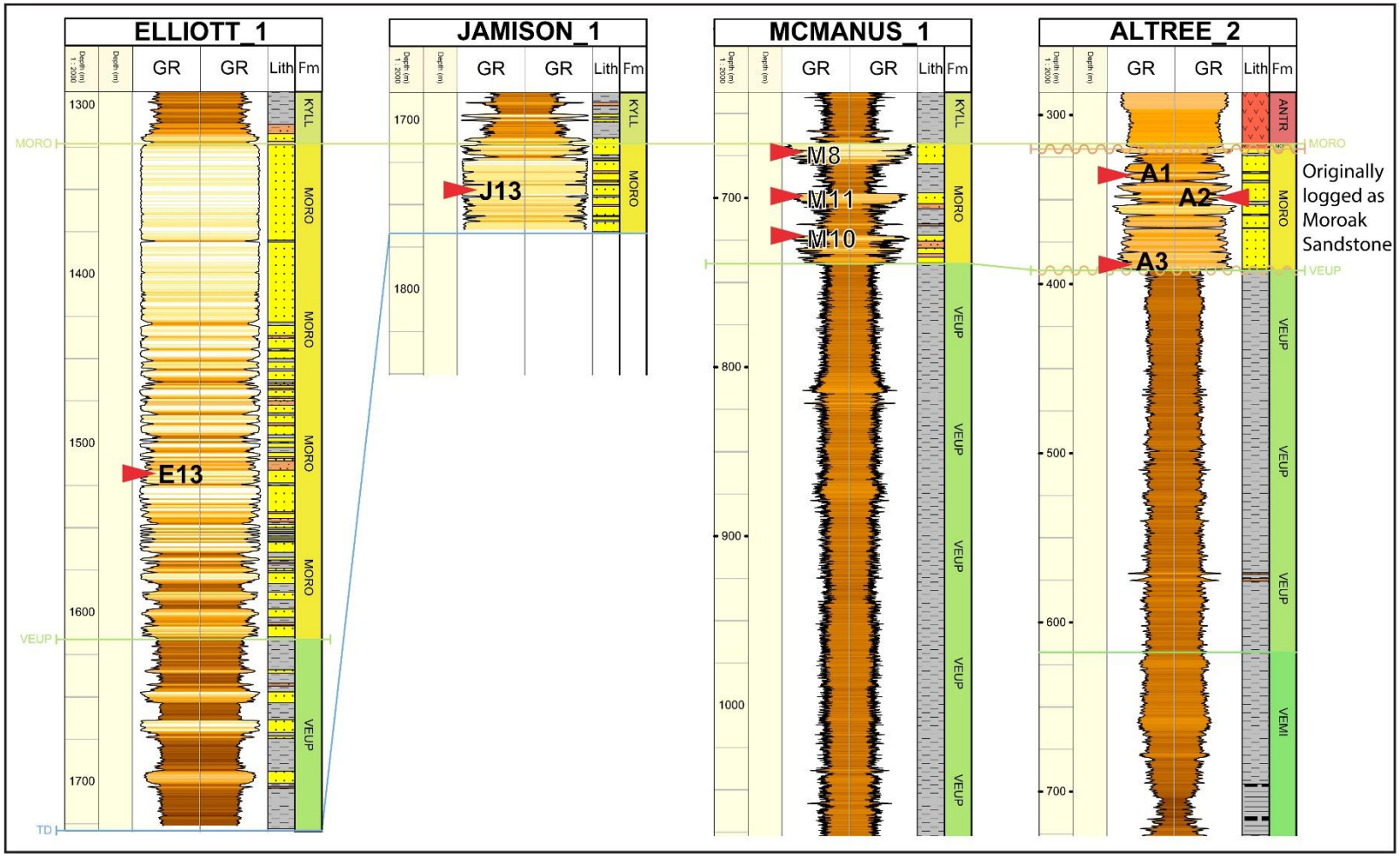

Figure 5: Vertically drilled exploration wells in the Beetaloo Basin that include the Moroak Sandstone; Elliott 1, Jamison 1, McManus 1 and Altree 2 (location in Fig.1), flattened to the top of the Moroak Sandstone formation. Note that this was the correlation before this study based on well completion reports. A result of this study has been to reassign the sandstone in Altree 2 to younger formations (see Fig. 6). GR log (mirrored), depth (m), Lith = lithology, Fm = formation, ANTR = Antrim Plateau Volcanics, KYLL = Lower Kyalla Formation, MORO = Moroak Sandstone, VEUP = Upper Velkerri Formation,

VEMI = Middle Velkerri Formation, TD = Total depth of hole, wavy line = unconformity. Samples labelled and marked by a red arrow. Note: Sever 1 was not cored through the Moroak Sandstone, and Walton 2 had no Moroak Sandstone. Thickness of Moroak Sandstone in wells: Elliott 1 - 318.72m, Jamison 1 - at least 52.53m, McManus 1 – 70.20m.

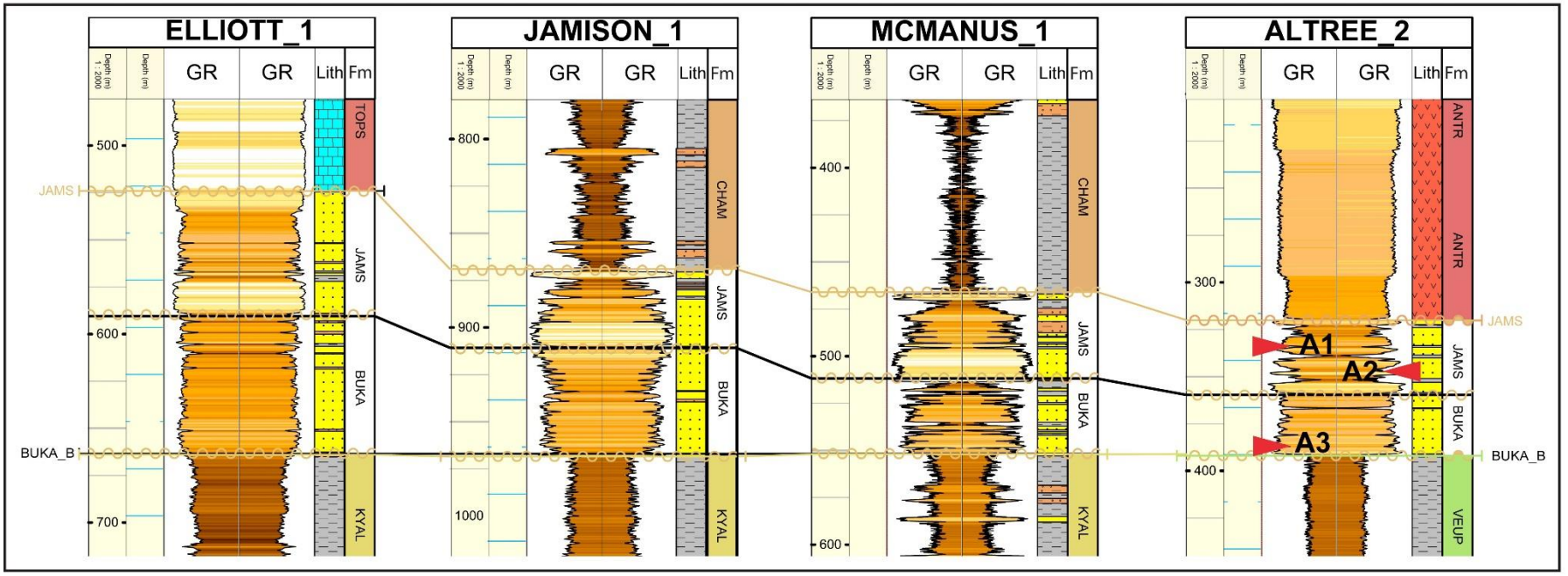

Figure 6: Vertically drilled exploration wells in the Beetaloo Basin that include the Jamison Sandstone and Bukalorkmi Sandstone; Elliott 1, Jamison 1, McManus 1, Walton 2 and Altree 2 (location in Fig. 1), flattened to the bottom of Bukalorkmi Sandstone. Note that Altree 2 - 320.0 to 391.72m was originally interpreted as Moroak Sandstone, I have reinterpreted as Jamison Sandstone and Bukalorkmi Sandstone, based on detrital zircon data and sequence boundary interpretation by Gorter and Grey (2012). GR log (mirrored), depth (m), Lith = lithology, Fm = formation, TOPS = Top Spring (Tindall) Limestone, CHAM = Chambers River Formation, ANTR = Antrim Plateau Volcanics, JAMS = Jamison Sandstone, BUKA = Bukalorkmi Sandstone, KYAL = Upper Kyalla Formation, VEUP = Upper Velkerri Formation, wavy line = unconformity. Samples labelled and marked by a red arrow.

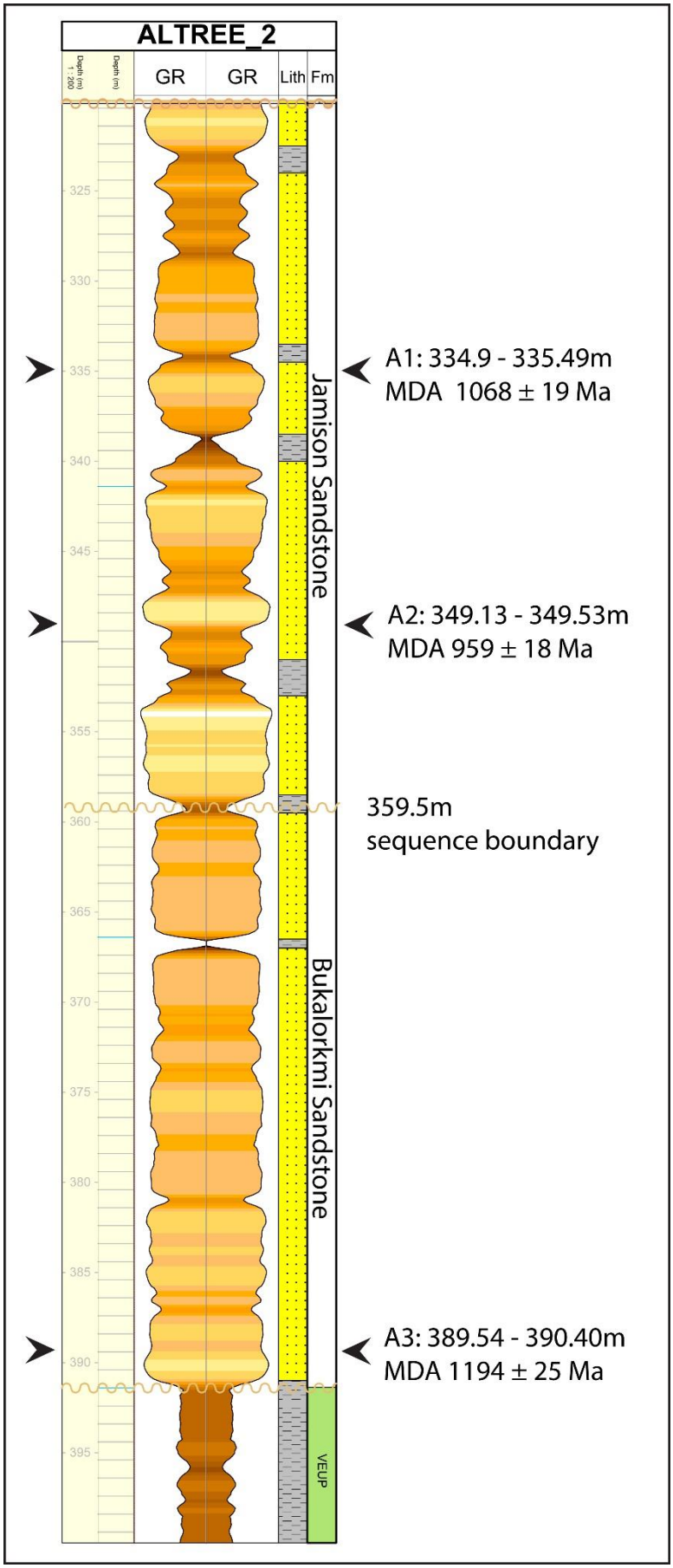

Figure 7: Vertically drilled exploration well Altree 2 (location in Fig. 1), the Moroak Sandstone was originally logged as 71.72m thick (320.0-391.72m), I have re-interpreted the Moroak Sandstone in Altree 2 to Bukalorkmi Sandstone 359.5m to 391.72m, and Jamison Sandstone 320.0m to 359.5m, based on detrital zircon data and extrapolation of sequence boundary interpretation by Gorter and Grey (2012). GR log (mirrored), depth (m), Lith = lithology, Fm = formation, VEUP = Upper Velkerri Formation, wavy line = unconformity. Samples labelled, marked by a black arrow and MDA = maximum deposition age, is the $^{238}U/^{206}Pb$ age (2σ error).

METHODS

Sandstone samples were obtained from six drillcore; Sever 1, Walton 2, Altree 2, McManus 1, Jamison 1 and Elliott 1, stored at the Darwin core library, Northern Territory, Australia (well logs: Figs. 4, 5, 6, 7). Sandstone sample size ranged from 19-75cm. Zircons were separated from host sandstones via crushing and milling, the disaggregated material was sieved to separate out the potential zircon component. The zircon component was panned to remove light mineral fractions and concentrate the heavy mineral fraction, via standard flotation and magnetic techniques. The zircon component was processed through high density heavy liquid (lithium heteropolytungstates) to further remove light mineral fractions.

Zircons were identified under a binocular microscope, picked by hand and mounted on epoxy discs, polished and carbon coated, prior to imaging using cathodoluminescence (CL) at the University of Adelaide, South Australia captured on the Quanta 600 Scanning Electron Microscope (SEM), a tungsten SEM fitted with a Gatan CL detector. CL images were used to determine zircon structure, so the core could be targeted.

U-Pb Detrital Zircon Geochronology

Analysis of detrital zircon obtained U-Pb ages using laser ablation ICP-MS with cation analysis (UP-213NdYag New Wave pulsed solid state laser coupled with Agilent 7500cx ICP- Quadrupole Mass Spectrometer) and the method described by Payne et al. (2010). U–Pb zircon geochronology was achieved using the LA-ICP-MS at the University of Adelaide. Laser settings were 30µm spot size, frequency 5 Hz with an intensity at 70%, ablation for 30 seconds, targeting mainly zircon cores. Data collected were corrected using Iolite (Chew et al., 2014). Concordia plots were created using Isoplot 3.00 in Excel (Ludwig, 2003). Multidimensional Scaling (MDS) plots and multi

kernel distributions were created using R software package (Vermeesch, 2013), for statistical analysis. Ages of single analyses are quoted at 2 sigma level, the maximum deposition age is calculated from the youngest >95% concordant analysis within analytical uncertainty (Spencer et al., 2016). All zircon U-Pb near-concordant (90-110%) data are found in Table 3, Appendix B. Many data yielded Mesoproterozoic ages that are a part of geological time where $^{206}Pb/^{238}U$ ages become more precise than $^{207}Pb/^{206}Pb$ ages, due to the differing half lives of ^{238}U and ^{235}U. I followed Nemchin and Cawood (2005) here in quoting the age with the lowest error as the best estimate of the grains age. For further detail refer to the extended method in the Appendix D.

OBSERVATIONS AND RESULTS

Sample localities are illustrated in Fig. 1, LA-ICP-MS U-Pb data are presented in Fig. 8, and Table 3 of the Appendix. U–Pb concordia plots are displayed in Fig. 8, kernel density plots are displayed in Fig. 10, and maximum deposition age defined using $^{238}U/^{206}Pb$ age over the $^{207}Pb/^{206}Pb$ age for increased precision.

Table 1: Beetaloo Basin core sample details, intervals and age data of detrital zircon analysed.

Stratigraphic Unit	BCS	BCS	BCS	BCS	MS	MS	MS	MS	MS	BS	JS	JS
Drillcore	Sever 1	Walton 2	Walton 2	Altree 2	Elliott 1	Jamison 1	McManus 1	McManus 1	McManus 1	Altree 2	Altree 2	Altree 2
Sample ID	S1	W1	W2	A13	E13	J13	M8	M11	M10	A3	A1	A2
Sample interval (m)	1167.11-1167.53	1013.29-1013.60	1010.65-1010.92	1467.79-1468.19	1518.16-1518.44	1740.00-1740.37	670.82-671.01	700.27-700.47	724.34-724.56	389.54-390.40	334.90-335.49	349.13-349.53
Lithology	white MG QtzA	white FG QtzA	white FG QtzA	QtzA (mineral rich)	grey/red QtzA	clean QtzA	QtzA (min Glc)	QtzA (min Py & Glc)	X-bd QtzA (min Py)	VC lithic Cong	CG QtzA	CG QtzA
No. of analyses	176	73	79	109	164	115	106	122	4	91	111	197
No. concordant (90-110%)	90	46	28	53	83	43	21	18	0	33	44	70
Major detritus peaks (Ma)											1120	1140
	1550			1580		1565	1590			1435	1535	1555
				1620								
	1725	1745	1785		1715	1745	1760	1730				
	1830	1840				1880						
	2490	2500		2420	2400							
YCZ* age (Ma ±2σ error)	1386 ± 13	1515 ± 16	1594 ± 13	1411 ± 20	1512 ± 28	1375 ± 15	1499 ± 34	1496 ± 25	N/A	1194 ± 25	1068 ± 19	959 ± 18
YCZ** age (Ma ±2σ error)	1354 ± 14	1579 ± 27	1669 ± 19	1409 ± 42	1550 ± 57	1404 ± 28	1569 ± 57	1527 ± 45	N/A	1237 ± 76	1092 ± 55	987 ± 68

YCZ = Youngest Concordant Zircon: * = $^{238}U/^{206}Pb$, ** = $^{207}Pb/^{206}Pb$, ages displayed are not necessarily the same grain. BCS = Bessie Creek Sandstone, MS = Moroak Sandstone, BS = Bukalorkmi Sandstone, JS = Jamison Sandstone, QtzA = quartz arenite, Cong = quartz rich conglomerate, FG = fine grained, MG = medium grained, CG = coarse grained, VC = very coarse grained, X-bd = cross-bedded, Py = pyrite, Glc – glauconite, min = minor. Major peaks are coloured, blue = Mesoproterozoic, red = Palaeoproterozoic.

Bessie Creek Sandstone

Sever 1 – Sample S1

In Sever 1, the Bessie Creek Sandstone was logged as 60.69m thick (1166.96-1227.65m). One sample was collected, a white medium grained quartz arenite (minor pyrite nodules and minor very fine biotite veins) from 1167.11-1167.53m, which was 0.15m below the top of the formation. Zircon grain morphology ranged from elongated to well rounded, abraded and fractured to euhedral, grain sizes ranged from ca. 90-220μm.

One hundred and seventy six zircon grains were analysed for U-Pb, yielding 90 >90% concordant zircons ranging in age from ca. 3443 Ma to ca. 1354 Ma ($^{207}Pb/^{206}Pb$ age), 71% were Palaeoproterozoic (Fig. 8). The youngest >95% concordant analysis within analytical uncertainty yielded a $^{238}U/^{206}Pb$ age of 1386 ± 13 Ma (2σ error), which I interpret as the maximum deposition age of this sample. Clusters of detrital zircon (>90% concordant) occurred at ~2490 Ma (ca. 2618-2393 Ma, 13%), ~1830 Ma (ca. 1944-1809 Ma, 21%), ~1725 Ma (ca. 1802-1643 Ma, 41%) and ~1550 Ma (ca. 1598-1505 Ma, 12%).

Walton 2 – Samples W1, W2

In Walton 2, the Bessie Creek Sandstone was logged as at least 49.5m thick (969.7-1019.2m, which was the end of hole). Two samples were collected; W1 was a white fine grained quartz arenite (minor very fine biotite veins) from 1013.29-1013.6m, which was 43.59m below the top of the formation and W2 was a white quartz arenite (minor

very fine biotite veins) from 1010.65-1010.92m, which was 40.95m below the top of the formation.

W1

Zircon grain morphology ranged from elongated to well rounded, abraded and fractured to euhedral, grain sizes ranged from ca. 80-220µm. Seventy three zircon grains were analysed for U-Pb, yielding 46 >90% concordant zircons ranging in age from ca. 3505 Ma to ca. 1579 Ma ($^{207}Pb/^{206}Pb$ age), 89% were Palaeoproterozoic (Fig. 8). The youngest >95% concordant analysis within analytical uncertainty yielded a $^{238}U/^{206}Pb$ age of 1515 ± 16 Ma (2σ error), which I interpret as the maximum deposition age of this sample. Clusters of detrital zircon (>90% concordant) occurred at ~2500 Ma (ca. 2539-2420 Ma, 17%), ~1840 Ma (ca. 1860-1805 Ma, 20%) and ~1745 Ma (ca. 1784-1697 Ma, 41%).

W2

Zircon grain morphology ranged from elongated to well rounded, abraded and fractured to euhedral, grain sizes ranged from ca. 70-230µm. Seventy nine zircon grains were analysed for U-Pb, yielding 28 >90% concordant zircons ranging in age from ca. 3351 Ma to ca. 1539 Ma ($^{207}Pb/^{206}Pb$ age), 82% were Palaeoproterozoic (Fig. 8). The youngest >95% concordant analysis within analytical uncertainty yielded a $^{238}U/^{206}Pb$ age of 1594 ± 13 Ma (2σ error), which I interpret as the maximum deposition age of this sample. The dominant cluster of detrital zircon (>90% concordant) occurred at ~1785 Ma (ca. 2147-1539 Ma, 86%).

Altree 2 – Sample A13

In Altree 2, the Bessie Creek Sandstone was logged as 417.46m thick (1229.65-1647.11m). One sample was collected, a quartz arenite (heavy mineral rich) from 1467.79-1468.19m, which was 238.14m below the top of the formation. Zircon grain morphology ranged from elongated to well rounded, abraded and fractured to euhedral, grain sizes ranged from ca. 50-180µm.

One hundred and nine zircon grains were analysed for U-Pb, yielding 53 >90% concordant zircons ranging in age from ca. 2987 Ma to ca. 1409 Ma ($^{207}Pb/^{206}Pb$ age), 57% were Palaeoproterozoic (Fig. 8). The youngest >95% concordant analysis within analytical uncertainty yielded a $^{238}U/^{206}Pb$ age of 1411 ± 20 Ma (2σ error), which I interpret as the maximum deposition age of this sample. Clusters of detrital zircon (>90% concordant) occurred at ~2420 Ma (ca. 2476-2255 Ma, 9%), ~1620 Ma (ca. 1805-1601 Ma, 47%) and ~1580 Ma (ca. 1598-1409 Ma, 42%).

Moroak Sandstone

Elliott 1 – Sample E13

In Elliott 1, the Moroak Sandstone was logged as 318.72m thick (1322.28-1641.0m). One sample was collected, a grey/red quartz arenite from 1518.16-1518.44m, which was 195.88m below the top of the formation. Zircon grain morphology ranged from elongated to well rounded, abraded and fractured to euhedral, grain sizes ranged from ca. 100-210µm.

One hundred and sixty four zircon grains were analysed for U-Pb, yielding 83 >90% concordant zircons ranging in age from ca. 3159 Ma to ca. 1383 Ma ($^{207}Pb/^{206}Pb$ age), 78% were Palaeoproterozoic (Fig. 8). The youngest >95% concordant analysis within

analytical uncertainty yielded a $^{238}U/^{206}Pb$ age of 1512 ± 18 Ma (2σ error), which I interpret as the maximum deposition age of this sample. Clusters of detrital zircon (>90% concordant) occurred at ~2420 Ma (ca. 2526-2172 Ma, 12%) and ~1715 Ma (ca. 1987-1383 Ma, 86%).

Jamison 1 – Sample J13

In Jamison 1, the Moroak Sandstone was logged as at least 52.53m thick (1714.32-1766.85m, which is the end of hole). One sample was collected, a clean quartz arenite from 1740-1740.37m, which was 25.68m below the top of the formation. Zircon grain morphology ranged from elongated to well rounded, abraded and fractured to euhedral, grain sizes ranged from ca. 90-250µm.

One hundred and fifteen zircon grains were analysed for U-Pb, yielding 43 >90% concordant zircons ranging in age from ca. 2498 Ma to ca. 1404 Ma ($^{207}Pb/^{206}Pb$ age), 77% were Palaeoproterozoic (Fig. 8). The youngest >95% concordant analysis within analytical uncertainty yielded a $^{238}U/^{206}Pb$ age of 1375 ± 15 Ma (2σ error), which I interpret as the maximum deposition age of this sample. Clusters of detrital zircon (>90% concordant) occurred at ~1880 Ma (ca. 1886-1865 Ma, 9%), ~1745 Ma (ca. 1820-1655 Ma, 63%) and ~1565 Ma (ca. 1641-1404 Ma, 26%).

McManus 1 – Samples M8, M10, M11

In McManus 1, the Moroak Sandstone was logged as 70.2m thick (668.0-738.2m). Three samples were collected; M8 is a quartz arenite (minor glauconite) from 670.82-671.01m, which was 2.82m below the top of the formation, M10 is a cross-bedded quartz arenite (minor pyrite nodules) from 724.34-724.56m, which was 56.34m below

the top of the formation, M11 is a quartz arenite (minor pyrite nodules and glauconite) from 700.27-700.47m, which was 32.27m below the top of the formation.

M8

Zircon grain morphology ranged from elongated to well-rounded, abraded and fractured to euhedral, grain sizes ranged from ca. 50-150µm. One hundred and six zircon grains were analysed for U-Pb, yielding 21 >90% concordant zircons ranging in age from ca. 2871 Ma to ca. 1538 Ma ($^{207}Pb/^{206}Pb$ age), 71% were Palaeoproterozoic (Fig. 8). The youngest >95% concordant analysis within analytical uncertainty yielded a $^{238}U/^{206}Pb$ age of 1499 ± 34 Ma (2σ error), which I interpret as the maximum deposition age of this sample. Clusters of detrital zircon (>90% concordant) occurred at ~1760 Ma (ca. 1821-1649 Ma, 68%) and ~1590 Ma (ca. 1597-1538 Ma, 23%).

M10

Zircon grain morphology ranged from elongated to sub-rounded, abraded and fractured to euhedral, grain sizes ranged from ca. 70-100µm, much smaller than zircon grains from E13 and J13. Four zircon grains were analysis for U-Pb, yielding no >90% concordant zircons, therefore I was unable to determine maximum deposition age for this sample.

M11

Zircon grain morphology ranged from elongated to well-rounded, abraded and fractured to euhedral, grain sizes ranged from ca. 50-100µm. One hundred and twenty two zircon grains were analysed for U-Pb, yielding 18 >90% concordant zircons ranging in age from ca. 2654 Ma to ca. 1527 Ma ($^{207}Pb/^{206}Pb$ age), 83% were Palaeoproterozoic (Fig.

8). The youngest >95% concordant analysis within analytical uncertainty yielded a $^{238}U/^{206}Pb$ age of 1496 ± 25 Ma (2σ error), which I interpret as the maximum deposition age of this sample. The main cluster of detrital zircon (>90% concordant) occurred at ~1730 Ma (ca. 1978-1527 Ma, 94%).

Samples originally logged as Moroak Sandstone – Reinterpreted as Jamison Sandstone and Bukalorkmi Sandstone

Altree 2 – Samples A1, A2, A3

In Altree 2, the Moroak Sandstone was originally logged as 71.72m thick (320.0-391.72m), reinterpretation details are found in the discussion. Three samples were collected; A1 was a coarse grained quartz arenite from 334.90-335.49m, which was 14.9m below the top of the formation, A2 was a coarse grained quartz arenite from 349.13-349.53m, which was 29.13m below the top of the formation. The lowest sample was A3, a very coarse grained lithic quartz rich conglomerate from 389.54-390.40m, which was 69.54m below the top of the formation.

A1

Zircon grain morphology ranged from elongated to well-rounded, abraded and fractured to euhedral, grain sizes ranged from ca. 80-180µm. One hundred and eleven zircon grains were analysed for U-Pb, yielding 47 >90% concordant zircons ranging in age from ca. 2103 Ma to ca. 1092 Ma, 86% were Mesoproterozoic (Fig. 8). The youngest >95% concordant analysis within analytical uncertainty yielded a $^{238}U/^{206}Pb$ age of 1068 ± 19 Ma (2σ error), which I interpret as the maximum deposition age of this sample. Clusters of detrital zircon (>90% concordant) occurred at ~1535 Ma (ca. 1698-1370 Ma, 79%) and ~1120 Ma (ca. 1132-1092 Ma, 17%).

A2

Zircon grain morphology ranged from elongated to well-rounded, abraded and fractured to euhedral, grain sizes ranged from ca. 90-290µm. One hundred and ninety seven zircons grains were analysed for U-Pb, yielding 70 >90% concordant zircons ranging in age from ca. 2455 Ma to ca. 987 Ma, 81% were Mesoproterozoic (Fig. 8). The youngest >95% concordant analysis within analytical uncertainty yielded a $^{238}U/^{206}Pb$ age of 959 ± 18 Ma (2σ error), which I interpret as the maximum deposition age of this sample**.** Clusters of detrital zircon (>90% concordant) occurred at ~1555 Ma (ca. 1814-1323 Ma, 74%) and ~1140 Ma (ca. 1248-987 Ma, 25%).

A3

Zircon grain morphology ranged from elongated to well-rounded, abraded and fractured to euhedral, grain sizes ranged from ca. 90-200µm. Ninety one zircon grains were analysed for U-Pb, yielding 33 >90% concordant zircons ranging in age from ca. 2880 Ma to ca. 1183 Ma, 79% were Mesoproterozoic (Fig. 8). The youngest >95% concordant analysis within analytical uncertainty yielded a $^{238}U/^{206}Pb$ age of 1238 ± 20 Ma (2σ error), which I interpret as the maximum deposition age of this sample. The dominant cluster of detrital zircon (>90% concordant) occurred at ~1435 Ma (ca. 1641-1237 Ma, 97%).

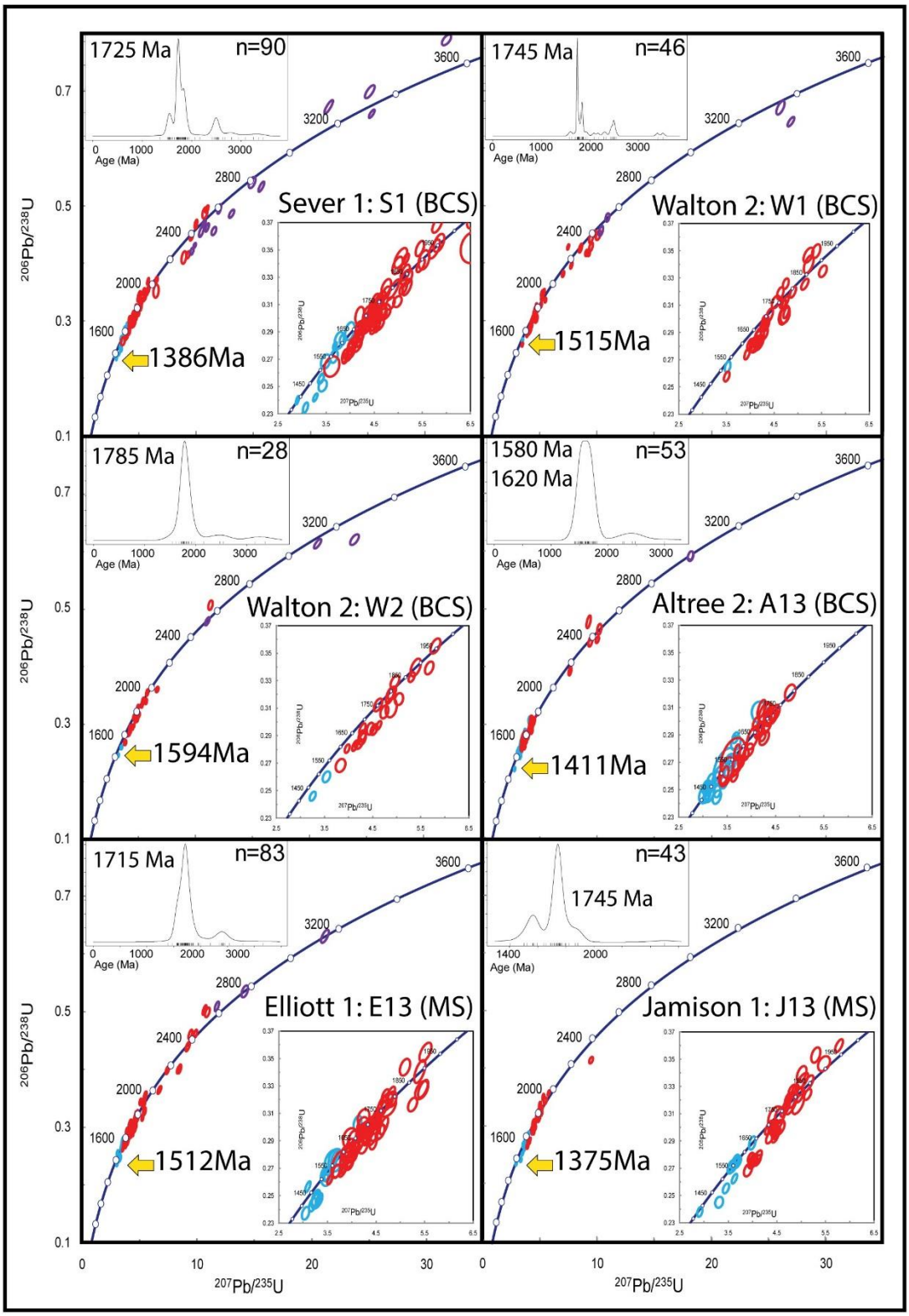
1725 Ma
n=90
Sever 1: S1 (BCS)
1386Ma
1745 Ma
n=46
Walton 2: W1 (BCS)
1515Ma
1785 Ma
n=28
Walton 2: W2 (BCS)
1594Ma
1580 Ma
1620 Ma
n=53
Altree 2: A13 (BCS)
1411Ma
1715 Ma
n=83
Elliott 1: E13 (MS)
1512Ma
n=43
1745 Ma
Jamison 1: J13 (MS)
1375Ma
Age (Ma)
206Pb/238U
207Pb/235U

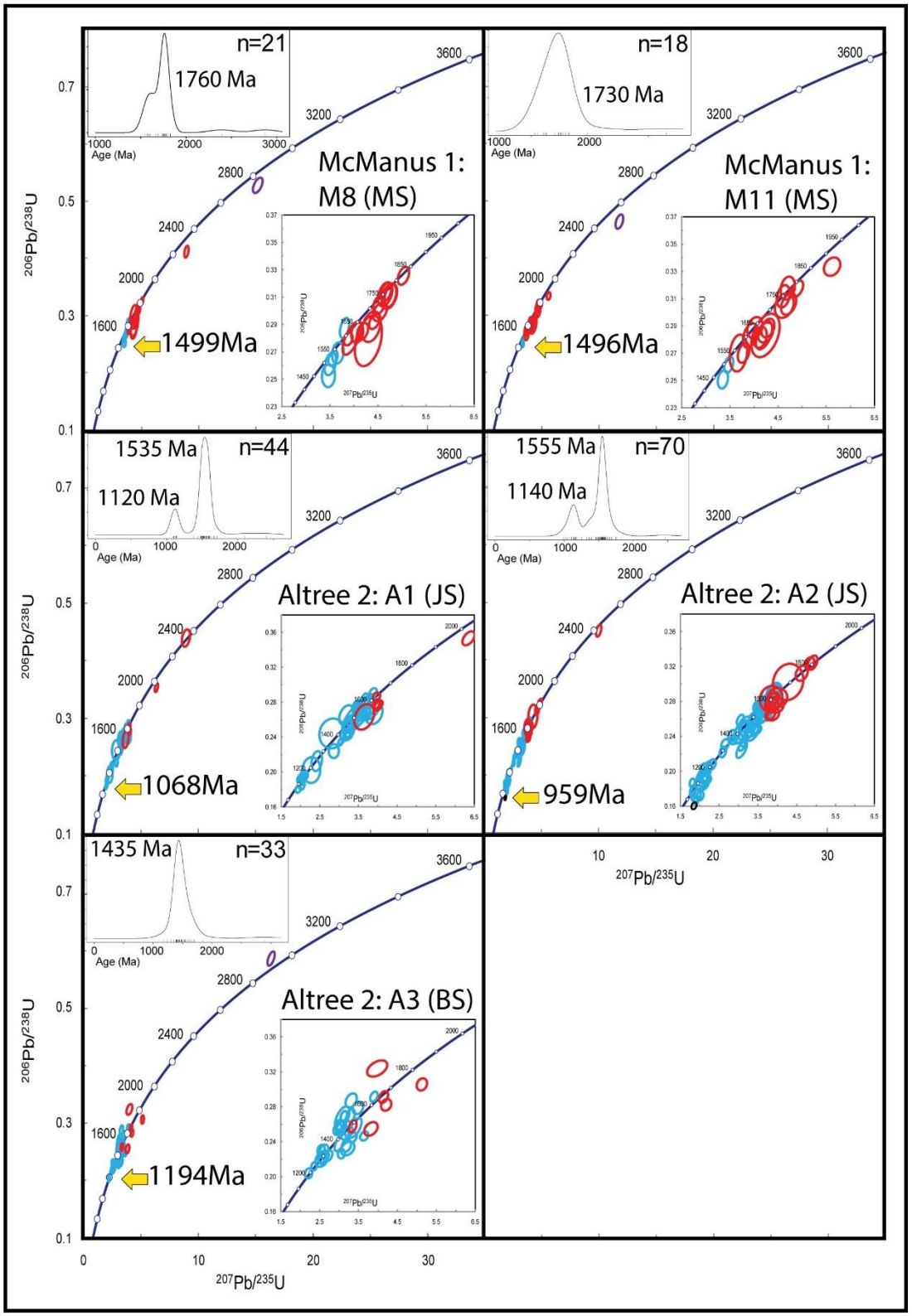

Figure 8: U–Pb concordia plots of 11 core samples taken from Beetaloo Basin, all >90% concordant data plotted, all data presented in Fig. 16 in Appendix A. Sample locations are illustrated in Fig. 1 and located in Table 1. Samples are labelled (drillcore, sample ID (bottom right), kernel density plots $^{207}Pb/^{206}Pb$ age data (top left), n = number of concordant analyses, >150 Ma 2 standard deviation removed, dominant peaks labelled. Data point error ellipses are 2 standard deviations. Data coloured based on $^{207}Pb/^{206}Pb$ age (Appendix B, Table 3), black = Neoproterozoic, blue =

Mesoproterozoic, red = Palaeoproterozoic, purple = Archaean. Maximum deposition age = yellow arrows are $^{238}U/^{206}Pb$ age (Ma). BCS = Bessie Creek Sandstone, MS = Moroak Sandstone, BS = Bukalorkmi Sandstone, JS = Jamison Sandstone. Note that all concordia plots display >90% concordance zircon data, while the maximum deposition age displayed is the youngest >95% concordance zircon analysis, refer to method for details.

DISCUSSION

Table 2: Summary of depositional age constraints of Maiwok Sub-Group sandstones analysed, in the Beetaloo Basin.

Stratigraphic Unit	Bessie Creek Sandstone	Moroak Sandstone	Bukalorkmi Sandstone	Jamison Sandstone
Maximum depositional age ($^{238}U/^{206}Pb$ age)	1386 ± 13 Ma	1375 ± 15 Ma	1194 ± 25 Ma	959 ± 18 Ma
Minimum depositional age	1324 ± 8 Ma*	513 ± 12 Ma**	513 ± 12 Ma**	513 ± 12 Ma**

Maximum depositional age and minimum depositional age are ± 2σ error level.
* from the Abbott et al. (2001) dated Derim Derim Dolerite.
** from Hanley and Wingate (2000) Antrim Plateau Volcanics.
Refer to discussion for details.

Depositional Age Constraints on the Maiwok Sub-Group

The maximum depositional ages of the Maiwok Sub-group in each case have been constrained by the youngest >95% near-concordant detrital zircon analysis from each formation. The majority of detritus displayed magmatic oscillatory zoning. Note that I have increased from the concordance requirement of >90% concordance, used for spectra comparison to >95% concordance, for the maximum depositional ages constraint. I did this to decrease the uncertainty on constraints and improve precision. The minimum deposition age constraint for the Bessie Creek Sandstone is constrained by the age of cross cutting of the Derim Derim Dolerite.

The Bessie Creek Sandstone sits conformably on the Corcoran Formation and conformably beneath the Velkerri Formation (Figs. 3, 4). The Velkerri Formation was cross-cut by dolerite in drillcore Sever 1 and Walton 2. This is correlated to the Derim Derim Dolerite, based on well reports descriptions (Torkington & Lanigan, 1991; Ledlie & Weste, 1989) and the description of the Derim Derim Dolerite by Smith (2015),

equivalent grain size, colour and mineralogy. The Derim Derim Dolerite is dated to 1324 ± 8 Ma (2σ error) by Abbott et al. (2001).

The minimum deposition age constraint for formations above the Bessie Creek Sandstone are only constrained by the age of Antrim Plateau Volcanics, as there are no records in core of dolerites intruding into the Moroak Sandstone, the Bukalorkmi Sandstone or the Jamison Sandstone, in the Beetaloo Basin. Therefore minimum deposition age constraint for these formations is the Antrim Plateau Volcanics found in core overlying the Maiwok Sub-group, with the exception of Elliott 1 drillcore. The Antrim Plateau Volcanics is dated to 513 ± 12 Ma (2σ error) by Hanley and Wingate (2000).

Depositional Age Constraints on the Bessie Creek Sandstone Formation

Of the three cores analysed that contained Bessie Creek Sandstone, Sever 1 (sample S1) yielded the youngest near-concordant zircon analysis. The maximum depositional age for the Bessie Creek Sandstone is 1386 ± 13 Ma (2σ error, Table 2). This is almost identical to data by Munson et al. (in prep.), who constrained the maximum deposition age to be 1385 ± 116 Ma (2σ error), from Bessie Creek Sandstone cropping out in the Urapunga Region (Fig. 1). As discussed above the Derim Derim Dolerite, dated to be 1324 ± 8 Ma (Abbott et al., 2001), provides the minimum depositional age constraint. The Bessie Creek Sandstone Formation, therefore, is interpreted to have been deposited between 1386 ± 13 Ma and 1324 ± 8 Ma.

Depositional Age Constraints on the Moroak Sandstone Formation

Of the four cores analysed that contained Moroak Sandstone, Altree 2 (sample A2) yielded the youngest near-concordant zircon analysis. However the detrital zircon age

distribution of samples from Altree 2 (A1, A2 and A3) that had been logged as Moroak Sandstone Formation in the original well completion reports (Weste et al., 1988) yielded similar age distributions to those from the Bukalorkmi and Jamison Sandstone Formations of Yang et al. (in prep.) and Munson et al. (in prep.).

Therefore, I interpret the Altree 2 Moroak Sandstone samples (A1, A2 and A3) to have been originally misinterpreted. This is supported by well correlations shown in Figs. 5 and 6, and by extrapolating the interpreted sequence boundaries from Gorter and Grey (2012). Because of this, I have reassigned these samples to the Bukalorkmi Sandstone and Jamison Sandstone, and will discuss them separately below.

Of the true Moroak Sandstone samples analysed, Elliott 1 (sample E13) yielded the youngest near-concordant zircon analysis. The maximum depositional age for the Moroak Sandstone is 1375 ± 15 Ma (2σ error, Table 2). This is similar to data by Munson et al. (in prep.), who constrained the maximum deposition age to be 1406 ± 78 Ma (2σ error), from Moroak Sandstone cropping out in the Urapunga Region (Fig. 1). As discussed above the Antrim Plateau Volcanics, dated to be 513 ± 12 Ma (Hanley and Wingate, 2000), provides the minimum depositional age constraint. The Moroak Sandstone Formation, therefore, is interpreted to have been deposited between 1375 ± 15 Ma and 513 ± 12 Ma.

Interpreted Sequence Boundary between the Bukalorkmi Sandstone Formation and the Jamison Sandstone Formation

Gorter and Grey (2012) subdivided the Bukalorkmi Sandstone and the Jamison Sandstone in the Beetaloo Basin, which they based on an interpreted sequence boundary (Figs. 6, 7). The (lower) Bukalorkmi Sandstone was more radioactive, yielding a higher gamma log response than Jamison Sandstone, with a thin basal conglomerate (Gorter

and Grey, 2012). The (upper) Jamison Sandstone also has a basal conglomerate (not always easily observed in well logs), characterised by a density peak, indicating denser rocks in the conglomerate and/or a lower gamma response, due to the clean nature of the Jamison Sandstone deposited in a transgressive system (as sea level rises). Abbott et al. (2001) and Silverman et al. (2005) have stated that the Bukalorkmi Sandstone and Jamison Sandstone may be equivalent to each other, but did not have the evidence to confirm this. Munson et al. (in prep.) has defined the Jamison Sandstone as 'ungrouped' and has separated the Jamison Sandstone samples from Balmain 1 (Fig. 12) into the upper and lower, which I have relabelled as B-JS and B-BS, respectively.

The Moroak Sandstone logged in Altree 2 was originally misinterpreted (320.0-391.72m). Here I tentatively reinterpret 320.0m to 359.5m as Jamison Sandstone and 359.5m to 391.72m as Bukalorkmi Sandstone (Figs. 6, 7) because of difference in zircon age distributions and the gamma response in the gamma well log, but I acknowledge that this is only provisional until more work can be done.

Depositional Age Constraints on the Bukalorkmi Sandstone Formation

The one sample of the interpreted Bukalorkmi Sandstone Formation analysed, Altree 2 (sample A3), yielded its youngest near-concordant zircon analysis. The maximum depositional age for the Bukalorkmi Sandstone is 1194 ± 25 Ma (2σ error, Table 2). Munson et al. (in prep.), who constrained the maximum deposition age to be 1353 ± 44 Ma (2σ error), from Bukalorkmi Sandstone cropping out in the Urapunga Region, and 1130 ± 42 Ma (2σ error), from Balmain 1 drillcore (Fig. 1). The latter is more similar to my data. As discussed above the Antrim Plateau Volcanics, dated to be 513 ± 12 Ma (Hanley and Wingate, 2000), provides the minimum depositional age constraint. The

Bukalorkmi Sandstone Formation, therefore, is interpreted to have been deposited between 1194 ± 25 Ma and 513 ± 12 Ma, in the Beetaloo Basin.

Depositional Age Constrains on the Jamison Sandstone Formation

Of the two samples analysed, Altree 2 (sample A2) yielded the youngest near-concordant zircon analysis. The maximum depositional age for the Jamison Sandstone is 959 ± 18 Ma (2σ error, Table 2). This is similar to data by Yang et al. (in prep.), who constrained the maximum depositional age to be 1050 ± 34 Ma (2σ error), sampled from Elliott 1, and Munson et al. (in prep.), who constrained the maximum depositional age to 1113 ± 76 Ma (2σ error), from Balmain 1 drillcore. As discussed above the Antrim Plateau Volcanics, dated to be 513 ± 12 Ma (Hanley and Wingate, 2000), provides the minimum depositional age constraint. The Jamison Sandstone Formation, therefore, is interpreted to have been deposited between 959 ± 18 Ma and 513 ± 12 Ma, in the Beetaloo Basin.

It should be noted that in contrast to my data and interpretation, Yang et al. (in prep.) and Munson et al. (in prep.) did not find significant differences in detrital zircon age distributions between samples from above or below the proposed sequence boundary between the Bukalorkmi and Jamison Sandstone Formations. This emphasises that uncertainty must remain when considering whether the Bukalorkmi and Jamieson Sandstone Formations are different formations until more work is undertaken.

Maiwok Sub-Group Stratigraphic and Temporal Variations in Provenance

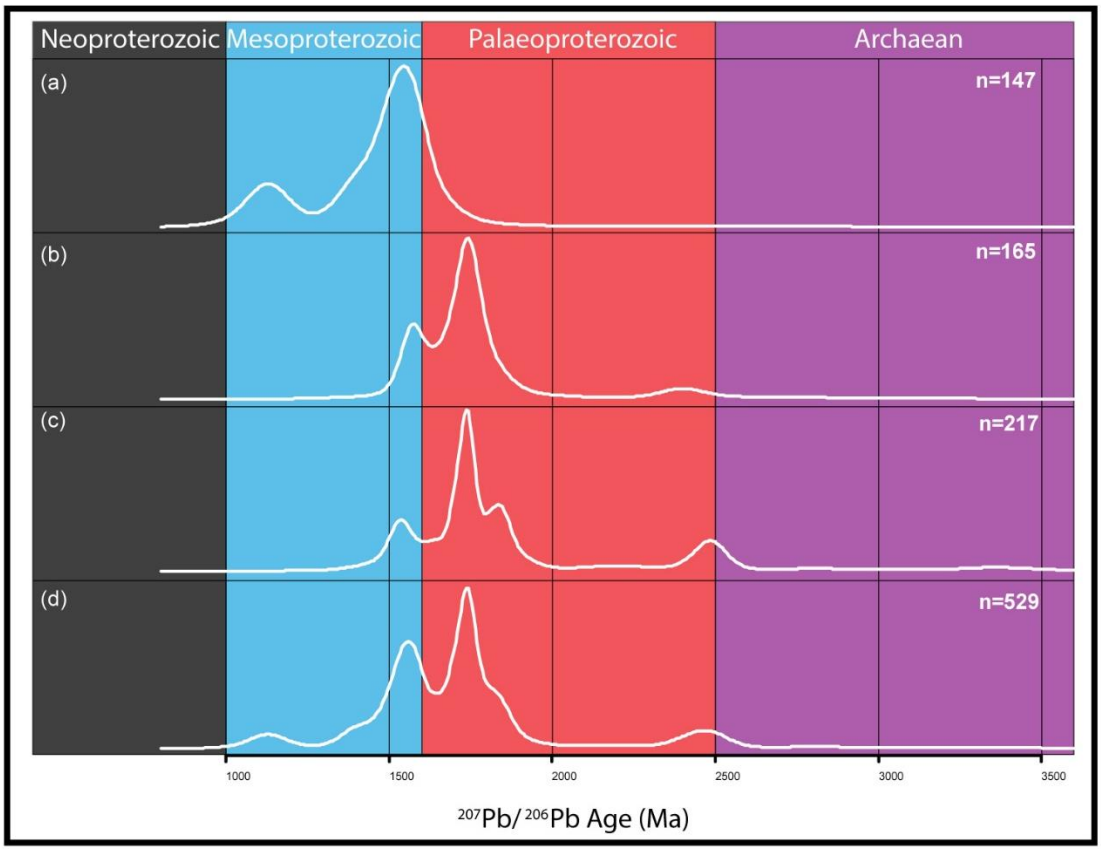

Figure 9: Kernel density plots of combined formation data in stratigraphic order, comparing age dated detrital zircon spectra (data sets of >90% concordant zircon $^{207}Pb/^{206}Pb$ ages); a) all combined Jamison Sandstone and Bukalorkmi Sandstone samples (Altree 2 originally logged as Moroak Sandstone; A1, A2, A3), b) all combined Moroak Sandstone samples (E13, J13, M8, M11), c) all combined Bessie Creek Sandstone samples (S1, W1, W2, A13), and d) all data combined. n = number of zircon analysis, plots created using Vermeesch (2013) software.

Combining all Bessie Creek Sandstone data (Fig. 9), yielded 217 near-concordant zircons ranging age between ca. 3505 Ma and ca. 1354 Ma ($^{207}Pb/^{206}Pb$ ages). Dominant clusters of detrital zircon occurred at ~1835 Ma (ca. 1972-1790 Ma, 21%) and ~1740 Ma (ca. 1784-1596 Ma, 42%).

Combining all Moroak Sandstone data (Fig. 9), yielded 165 near-concordant zircons ranging in age between ca. 3159 Ma and ca. 1383 Ma ($^{207}Pb/^{206}Pb$ ages). Dominant clusters of detrital zircon occurred at ~1745 Ma (ca. 1987-1640 Ma, 66%) and ~1575 Ma (ca. 1630-1383 Ma, 24%).

Data from all Jamison Sandstone and Bukalorkmi Sandstone samples were combined (Fig. 9), due to the low number of analysis for these formations. Combined data yielded 147 near-concordant zircons ranging in age between ca. 2880 Ma and ca. 987 Ma ($^{207}Pb/^{206}Pb$ ages). Dominant clusters of detrital zircon occurred at ~1545 Ma (ca. 1835-1301 Ma 79%) and ~1130 Ma (ca. 1248-987 Ma, 18%).

When comparing the differences from the Bessie Creek Sandstone to the Moroak Sandstone the Archaean peak decreases in magnitude, the ~1835 Ma peak vanishes and the early Mesoproterozoic peak gets younger from ca. 1596 to ca.1575 Ma. The dominant cluster from the Bessie Creek Sandstone and the Moroak Sandstone formations are equivalent, but becomes more dominant in the Moroak Sandstone formation at ~1740 Ma. The third dominant peak in the Bessie Creek Sandstone gets progressively younger up stratigraphy, the second dominant peak in the Moroak Sandstone and the dominant peak in the Jamison/Bukalorkmi Sandstone formations at ~1550 Ma, demonstrating a shift in the dominant provenance source. The second dominant cluster from the Jamison/Bukalorkmi Sandstone at ~1130 Ma, was not observed in the Bessie Creek Sandstone or the Moroak Sandstone, which demonstrates a new provenance source.

Maiwok Sub-Group Regional and Spatial Variations in Provenance

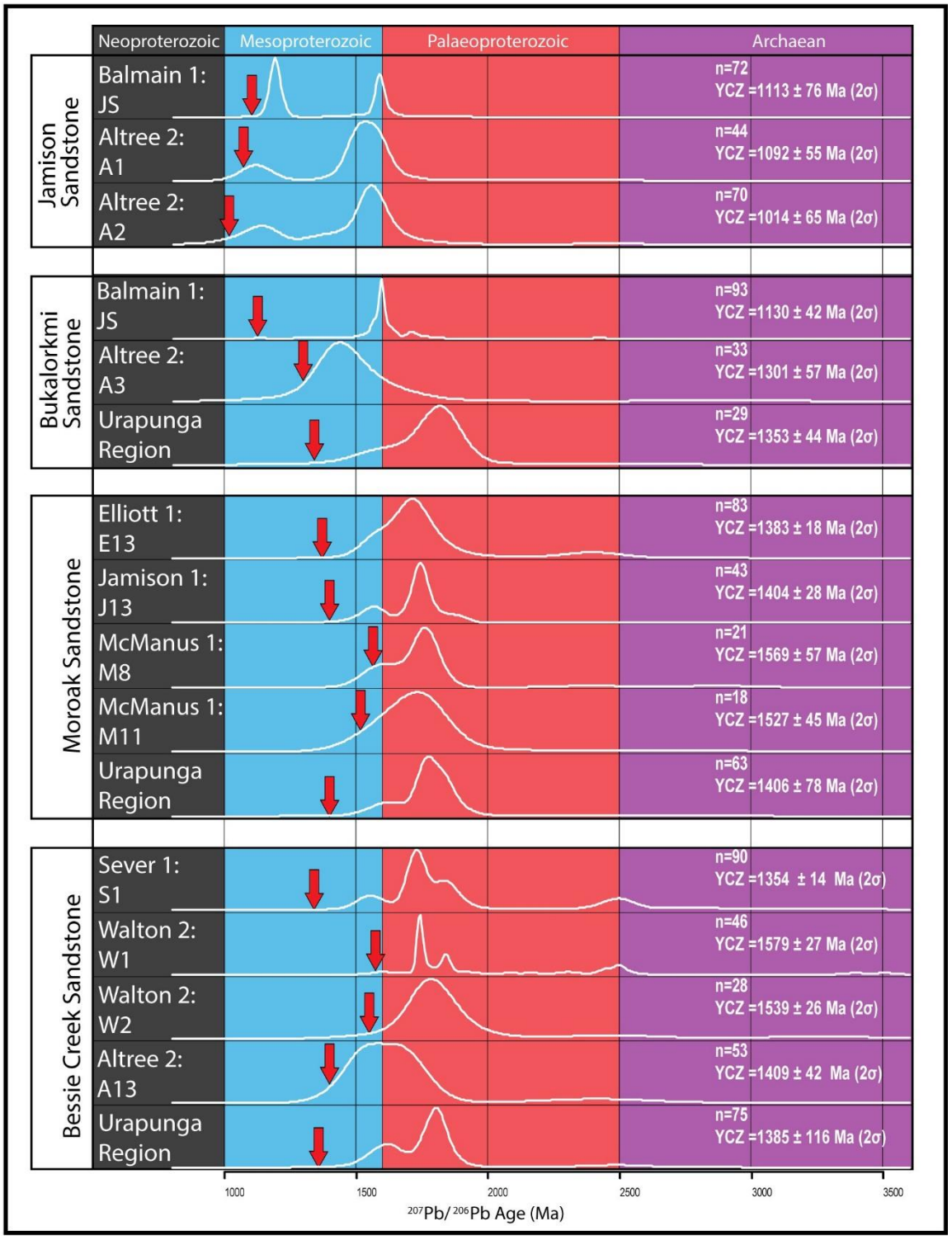

Figure 10: Kernel density plots comparing age dated detrital zircon spectra (data sets of >90% concordant zircon $^{207}Pb/^{206}Pb$ ages) of Maiwok Sub-group sandstones, arranged in stratigraphic order, in the Beetaloo Basin and Urapunga Region. Balmain1 and Urapunga Region spectra derived from data found in Munson et al., 2016. Red arrows indicate the YCZ (youngest concordant zircon) for each sample (2σ error), n = number of zircon analysis, plots created using Vermeesch (2013) software. Note that the YCZ indicated on this figure are $^{207}Pb/^{206}Pb$ ages and only within >90% concordance.

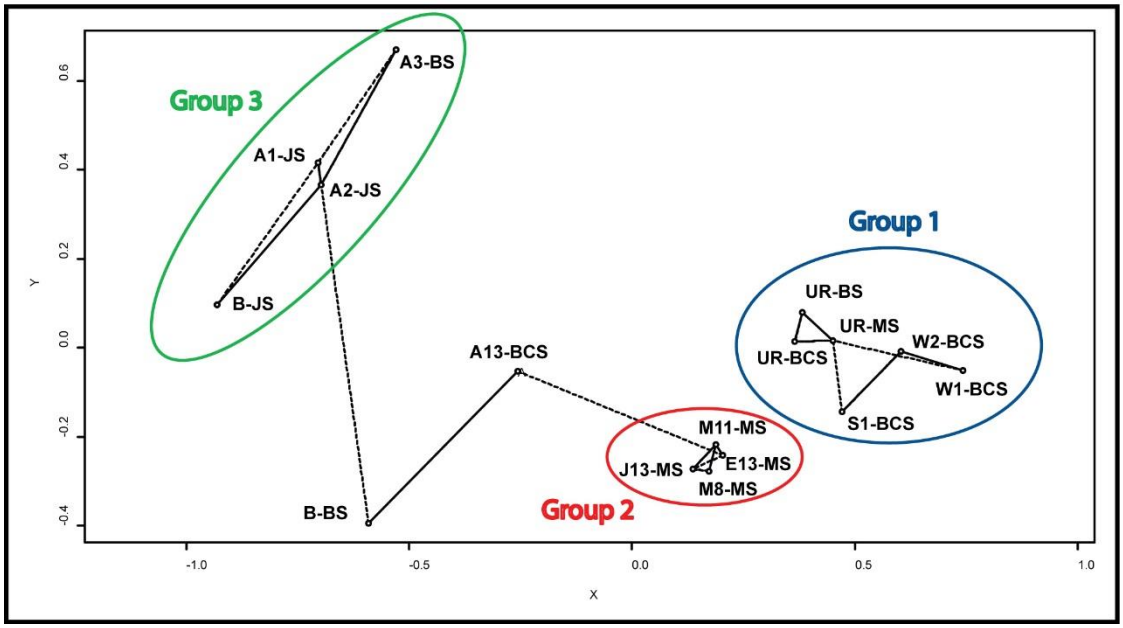

Figure 11: Map of dissimilarly – Multidimensional Scaling (MDS) plot of Beetaloo Basin and Urapunga Region data sets of >90% concordant zircon ages, similar samples cluster close together and dissimilar far apart, the closest neighbouring samples are connected with a solid line, the second closest with a dashed line (Vermeesch, 2013). Labelled: Sample ID and sample formation. UR = Urapunga Region, B = Balmain 1, BCS = Bessie Creek Sandstone, MS = Moroak Sandstone, BS = Bukalorkmi Sandstone, JS = Jamison Sandstone. Group 1; S1-BCS, W1-BCS, W2-BCS, UR-BCS, UR-MS, UR-BS, Group 2; M8-MS, M11-MS, J13-MS, E13-MS and Group 3; A1-JS, A2-JS, A3-BS, B-JS.

I have identified three main groups of detrital zircon spectra based on their similarities on Figure 11 that I have circled and labelled. Group 1 is dominated by Bessie Creek Sandstone samples (S1-BCS, W1-BCS, W2-BCS, UR-BCS, UR-MS, UR-BS), Group 2 is dominated by Moroak Sandstone samples (M8-MS, M11-MS, J13-MS, E13-MS) and Group 3 is dominated by Jamison Sandstone samples (A1-JS, A2-JS, A3-BS, B-JS). These groups are not restricted to stratigraphic formations.

Bessie Creek Sandstone

Kernel density curves for the Bessie Creek Sandstone core samples from Sever 1 (S1), Walton 2 (W1, W2) and outcrop Urapunga Region (UR-BCS) closely resemble each other, and major peak ages were equivalent (Table 1, Fig. 10). The Bessie Creek

Sandstone in Altree 2 (A13) was relatively thicker (Fig. 4) than Sever 1 or Walton 2 (Walton 2 was not drilled all the way through in the Bessie Creek Sandstone), and A13 was sampled deeper in the formation relative to the Velkerri Formation (compared to other Bessie Creek Sandstone samples), which may point to a stratigraphic variation and explain why it had such a distinctively different signature from Sever 1 and Walton 2. Walton 2 and Altree 2 were initially expected to be very similar due to the short 15km distance between them.

Sample A13 had a similar maximum deposition age to other Bessie Creek Sandstone samples but plotted in closer proximity to the samples of other formations that occur south of the Walton High (Fig. 12).

The two Walton 2 samples (W1 and W2) were only separated by 2.37 m and the well log suggests consistent sandstone between them (Fig. 5). Both samples had similar detrital zircon age spectra. Correlations made by comparing detrital zircon multidimensional scaling plot (Fig. 11) highlight the strong statistical similarities in zircon age distribution between Sever 1 and Walton 2. Urapunga Region samples provided by Munson et al. (2016), Bessie Creek Sandstone, Moroak Sandstone and Bukalorkmi Sandstone, are statistically most similar to each other in age distribution, and also share similarities with sandstones from Sever 1 and Walton 2 (Group 1). This suggests that there may be shared sources in this northern area independent of age of deposition.

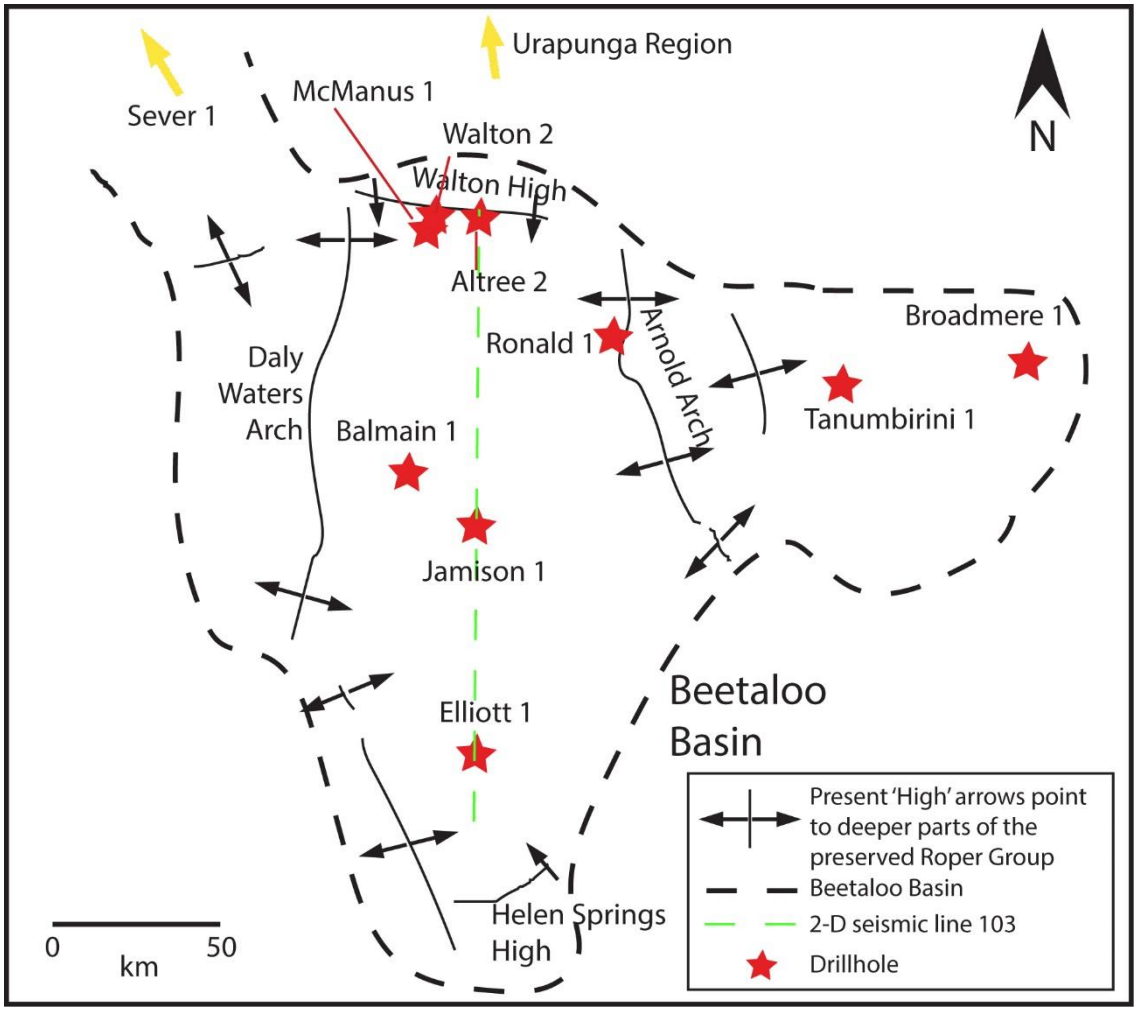

Figure 12: Simplified partial map of the Beetaloo Basin, showing major tectonic elements and drillholes. McManus 1, Walton 2 and Altree 2 all drilled in close proximity to the Walton High. Defined structures regional boundaries; Walton High, Daly Waters Arch (High), Arnold Arc and Helen Springs High, (redrafted after Silverman et al., 2005).

Moroak Sandstone

Kernel density curves for the Moroak Sandstone core samples from Elliott 1 (E13), Jamison 1 (J13) and McManus 1 (M8, M11) closely resemble each other, and major peak ages were equivalent (Table 1, Fig. 10). McManus 1 was vertically consistant between samples M8 and M11, spectra are equivalent, despite a possible change in sea-level, due to faulting, or possibly changing distributory channels and overbank deposits, lithology cycled; sand-shaly-sand-shaly (Fig. 5), with 29.26m separating samples.

Correlations made by comparing detrital zircon multidimensional scaling plot (Fig. 11), highlight the very strong statistical similarities/equivalents (via tight clustering) in age distribution between Elliott 1, Jamison 1 and McManus 1. This illustrates that the Moroak Sandstone was regionally consistent, extremely well sorted sheet sand, across the Beetaloo Basin. Outside the Beetaloo Basin, there was a significant provenance difference in the outcropping Urapunga Region - Moroak Sandstone sample (provided by Munson et al., 2016). Fig. 11 highlights the regional provenance variation between the Beetaloo Basin - Moroak Sandstone and the Urapunga Region - Moroak Sandstone, where the Walton High defines the boundary (Fig. 12) between samples in this study. Because of his regional provenance variation Urapunga Region - Moroak Sandstone, where excluded from Group 2, containing only Beetaloo Basin Moroak Sandstone.

Bukalorkmi Sandstone and Jamison Sandstone

Kernel density curves for Bukalorkmi Sandstone core samples from Altree 2 (A3) and samples provided by Munson et al. (in prep.); Balmain 1 (B-BS) and outcropping Urapunga Region - Bukalorkmi Sandstone (UR-BS) show considerable variation between the age spectra (Fig. 10).

The Urapunga Region - Bukalorkmi Sandstone also displayed a regional provenance variation (Fig. 11), due to the Walton High regional boundary.

Kernel density curves for Jamison Sandstone core samples from Altree 2 (A1, A2) and Balmain 1 (B-JS) provided by Munson et al. (in prep.) highlight the similarities between A1, A2 (Table 1) and B-JS (Fig. 10) with major peaks correlating visually, indicating these sample age distributions are similar.

Correlations made by comparing detrital zircon multidimensional scaling plot, highlight the strong statistical similarities in age distribution between A1 and A2. B-JS and A3

are more similar to A1 and A2 than to other samples, while B-BS is very weakly linked to A2, implying less similarity, which is why it was not included in Group 3 (Fig. 11).

Walton High as a Provenance Boundary

I interpret the Walton High as a provenance boundary between the north and south of the Beetaloo Basin (Fig. 12). Just south of the Walton High, in McManus 1 drillcore, the Kyalla Formation was 115.1m thick and the Moroak Sandstone was 70.2m thick, neither of these formations were found in drillcore from Altree 2 or Walton 2, only a few kilometres north of McManus 1. Also the depth to the top of the Velkerri Formation in McManus 1 drillcore was 738.2m, ca. 350-450m deeper than the Velkerri Formation in drillcore from Altree 2 (391.72m) or Walton 2 (259.6m). This apparent syn-depositional boundary is reflected in the detrital zircon age spectra (Fig. 10) and highlighted by grouping of samples (Fig. 11). I interpret the Walton High to be a syn-depositional fault that bounds the Beetaloo Basin, significantly affecting Roper Group formation thickness and separating provenance domains. It is likely that the Daly Waters High acted as a similar regional provenance constraint from east to west as well as the Helen Spring High regionally constraining provenance from south to north (opposite to the Walton High).

Provenance Sources of the Maiwok Sub-Group in the Beetaloo Basin

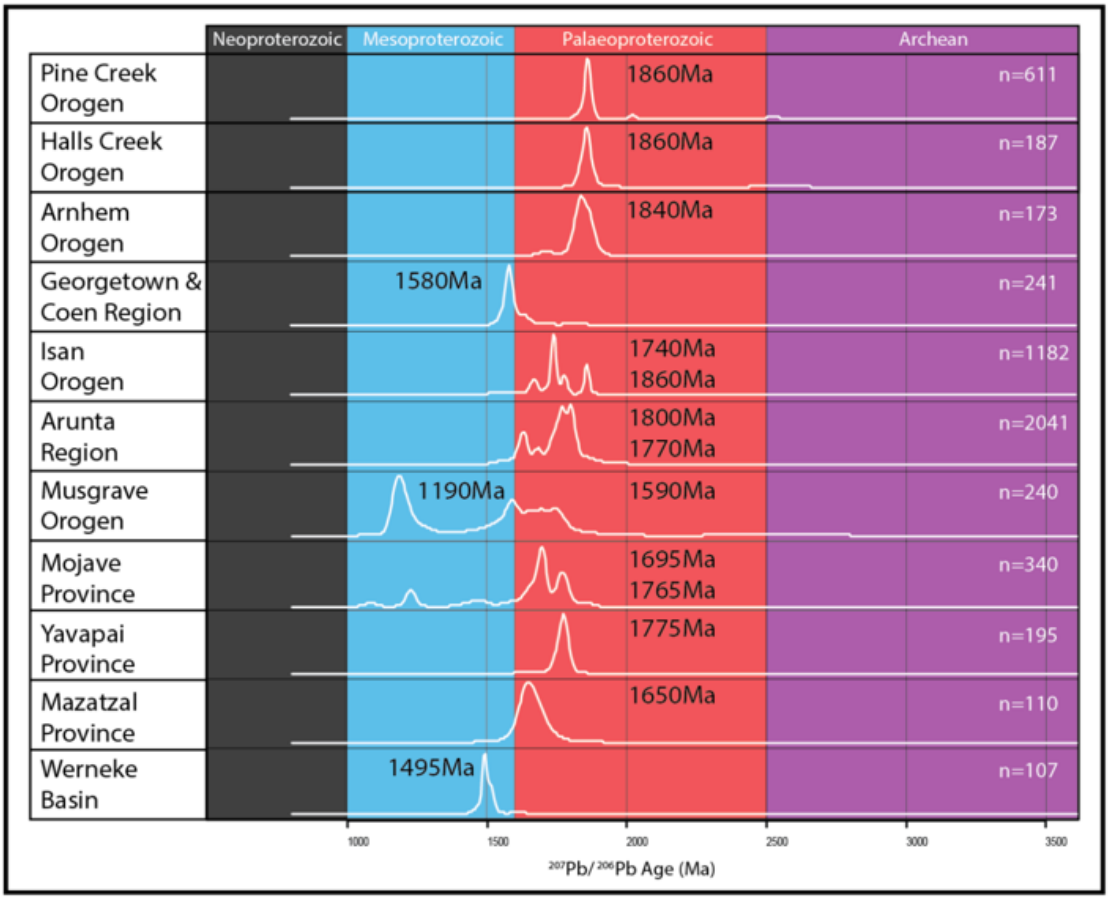

Figure 13: Kernel density plots comparing age dated detrital zircon spectra (data sets of >90% concordant zircon $^{207}Pb/^{206}Pb$ ages) of potential orogenic sources to the Beetaloo Basin. Spectra derived from tabulated; Pine Creek Province data from Worden et al. (2006), Worden et al. (2006b), Worden et al. (2008), Carson et al. (2009), Hollis et al. (2010), Beyer et al. (2013), Kositcin et al. (2013); Halls Creek Province data from Worden et al. (2008); Arnhem Province data from Kositcin et al. (2015); Georgetown & Coen Region data from Blewett et al. (1998), Hoskin et al. (2000), Kositcin et al. (2009); Mount Isa Province data from Page and Sun (1998), Neumann et al. (2006), Neumann et al. (2009), Cross et al. (2016); Arunta Region data from Cross et al. (2005), Cross et al. (2005b), Cross et al. (2005c), Worden et al. (2006), Worden et al. (2006b), Worden et al. (2008), Carson et al. (2009), Hollis et al. (2010), Beyer et al. (2013), Bodorkos et al. (2013), Kositcin et al. (2013), Kositcin et al. (2013b), Kositcin et al. (2014), Kositcin et al. (2014b), Kositcin et al. (2015b), Beyer et al. (2015), Beyer et al. (2016); Musgrave Province data from Wade (2006); Mojave Province data from Barth et al. (2000), MacLean, (2007), Barth et al. (2009), Mahon et al. (2014); Yavapai Province data from Mahon et al. (2014); Mazatzal Province data from Rämö et al. (2003), Amato et al. (2008); Werneke Basin data from Medig et al. (2014). Major peaks labelled (Ma), n= number of zircon analysis, plots created using Vermeesch (2013) software.

I have investigated the probable sediment pathways by comparing detrital sources to detrital zircons from all samples (combined) and detrital zircons of combined formations. Detritus from all eleven samples combined from this study, yielded early

Palaeoarchean to early Neoproterozoic ages (Fig. 9). When all data are combined, 529 near-concordant zircons range between ca. 3505 Ma and ca. 987 Ma ($^{207}Pb/^{206}Pb$ ages). Clusters of detrital zircon occur at ~2460 Ma (2662-2327 Ma, 8%), ~1720 Ma (1987-1640 Ma, 50%), ~1560 Ma (1636-1301 Ma, 36%), and ~1110 Ma (1248-987 Ma, 5%). The wide range of zircon clusters was expected, as they are detrital zircon, from a number of orogenic sources.

Detrital zircon deposited in the Beetaloo Basin, were most likely sourced from Australia, but according to the AUSWUS (Burrett & Berry, 2000) reconstruction (Fig. 2), Laurentian sources are also possible. Laurentia was predicted to be proximal to the North Australian Craton at the time of deposition of the Maiwok Sub-group ca. 1400-1000 Ma **(**Gibson et al., 2013; Medig et al., 2014**)** so based on this reconstruction, sources from Laurentia have been included in the study.

Detrital zircons from sedimentary assemblages in the Beetaloo Basin samples, point to contributions from potential provenance sources. Source data collected was sorted into regions (Fig. 13, Table 4) and compiled into kernel density plots, to identify dominant age population clusters to be compared to Beetaloo Basin samples (Fig. 9). I have made the assumption that the erosion of provenance terranes and subsequent sediment transportation to the Roper depocentre, facilitated the deposition of detritus in the Beetaloo Basin, which I have sampled. Comparisons made between source terranes and Beetaloo Basin samples were based on how similar they were to each other using a multidimensional scaling plot (Fig. 14) and the dominant peak range of magmatic zircon ages relating to orogenic events (Fig. 13), discussed below in terms of 'groups'. Groups highlight stratigraphic and regional provenance constraints.

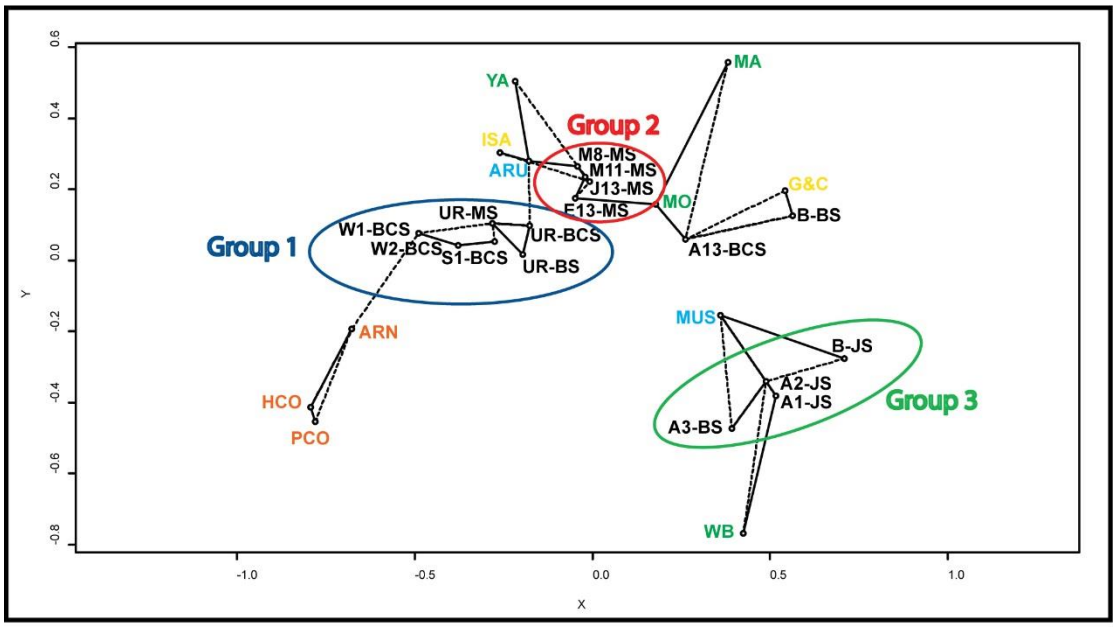

Figure 14: Map of dissimilarily – MDS plot of Beetaloo Basin, Urapunga Region and potential provenance source data sets of >90% concordant zircon ages, similar samples cluster close together and dissimilar far apart, the closest neighbouring samples are connected with a solid line, the second closest with a dashed line (Vermeesch, 2013). Sample ID and formation abbreviations are labelled. Black = Beetaloo Basin and Urapunga Region detrital zircon data, Orange = north and north-west orogenies, Blue = south orogenies, yellow = eastern orogenies, green = Laurentian/North American orogenies and Werneke Basin detrital data. Group 1; S1-BCS, W1-BCS, W2-BCS, UR-BCS, UR-MS, UR-BS, Group 2; M8-MS, M11-MS, J13-MS, E13-MS and Group 3; A1-JS, A2-JS, A3-BS, B-JS.

I have identified the same three main groups of detrital zircon spectra, based on their similarities on Figure 14, as in Figure 11. As previously stated, Group 1 is dominated by Bessie Creek Sandstone samples, Group 2 is dominated by Moroak Sandstone samples and Group 3 is dominated by Jamison Sandstone samples, these groups are not restricted to stratigraphic formations.

Provenance source terranes to the north of the Beetaloo Basin, Pine Creek Province (PCO), Halls Creek Province (HCO) and Arnhem Province (ARN) share similarities to Group 1. These northern sources are characterised by the age range ca. 1900-1800 Ma, which correspond to the Nimbuwah Event (PCO; Ahmad and Scrimgeour, 2013), the

Halls Creek Orogen (HCO; Ahmad and Scrimgeour, 2013) and the Arnhem Orogen (ARN; Ahmad and Scrimgeour, 2013).

Provenance source terranes to the east and south of the Beetaloo Basin, Mount Isa Province (ISA), and Arunta Region (ARU) also share similarities to Group 1 and Group 2. These sources are characterised by the age range ca. 1800-1700 Ma, which corresponds to the Big Event from the Mount Isa Province (Scott et al., 1998), and the Yambah Event and Strangways Orogeny from the Arunta Region (Ahmad and Scrimgeour, 2013). The Mount Isa Province and Arunta Region were also characterised by the age range ca. 1600-1500 Ma, which correspond to the Isan Orogeny from the Mount Isa Province (Jackson et al., 1999), and the Chewings Event from the Arunta Region (Ahmad and Scrimgeour, 2013).

Laurentian provenance source terranes (MO, YA, MA) from the Southeast of the Beetaloo Basin, also share similarities to Group 2. These Laurentian sources are characterised by the age range ca. 1850-1650 Ma (Farmer et al., 2005) which correspond to the Mojave Province (MO), Yavapai Province (YA) and Mazatzal Province (MA). Due to the large range (ca. 200Ma), and the overlap of ranges with North Australian Craton sources, I am hesitant to confirm these Laurentian sources.

Group 3 was similar to the Musgrave Province, this provenance source terrane is south of the Beetaloo Basin. The arc magmatism relating to ocean closure between the South Australian Craton and the North Australian Craton, and the Musgrave Orogeny both from the Musgrave Province, are characterised by the age range ca. 1600-1540 Ma and ca. 1230-1150 Ma (Wade, 2006), respectively. These combined events correspond strongly to Group 3. Group 3 was also similar to the Werneke Basin from Laurentia.

This basin is not a source to Group 3, but possibly has a shared 'unknown' provenance source terrane.

Tectonic Setting of the Beetaloo Basin

As stated earlier, there are two main hypothesised tectonic settings to explain the basin type that the Roper Group was deposited in. For an orogenic flexure basin as Abbott and Sweet (2000) proposed, there would need to be a magmatically active source region adjacent to the basin.

The dominant provenance sources to the Bessie Creek Sandstone and Moroak Sandstone are from the Mount Isa Province and the Arunta Region. The Isan Orogen from the Mount Isa Province was ca. 200-240 Ma older than the age of deposition. The Anmatjira Uplift from the Arunta Region was ca. 75-125 Ma older than the age of deposition. Therefore these provenance areas were not magmatically active at the time of deposition. Because of this, the orogenic flexure loading basin model was less likely at the time of deposition of the Bessie Creek Sandstone and Moroak Sandstone in the Beetaloo Basin. This suggests of the two models, the extension/sag basin proposed by Betts and Giles (2006) is more likely.

However, the dominant provenance source to the Bukalorkmi Sandstone and Jamison Sandstone was the Musgrave Province. The Musgrave Province had both felsic and mafic intrusions that were magmatically active (Wade, 2006), during period of deposition of the Bukalorkmi Sandstone and Jamison Sandstone. The Musgrave Province may have had some control on the formation of the Bukalorkmi Sandstone and Jamison Sandstone. Possibly resulting in the down warping the Beetaloo Basin, as a very low amplitude, long wavelength flexure. Similar cratonic areas have been proposed to show such low amplitude, long wavelength, warping forelandward orogens (Collins

et al., 2015), for example the Kurnool Group, in the Cuddapah Basin, India. If this was the case, then the Bukalorkmi Sandstone and Jamison Sandstone were syn-orogenic, deposited far in the foreland of the evolving Musgrave Orogeny. The Bukalorkmi Sandstone and Jamison Sandstone would be expected to be thicker to the south, and exhibit a wedge shape. Due to low number of samples analysed from the Bukalorkmi Sandstone and Jamison Sandstone, I am hesitant in discounting the extension basin setting. Also I have examined seismic line 103 trending north - south through the Beetaloo Basin (Fig. 15). No obvious thickening or a wedge shape of any Maiwok Sub-group formations, to the south of the Beetaloo Basin was observed.

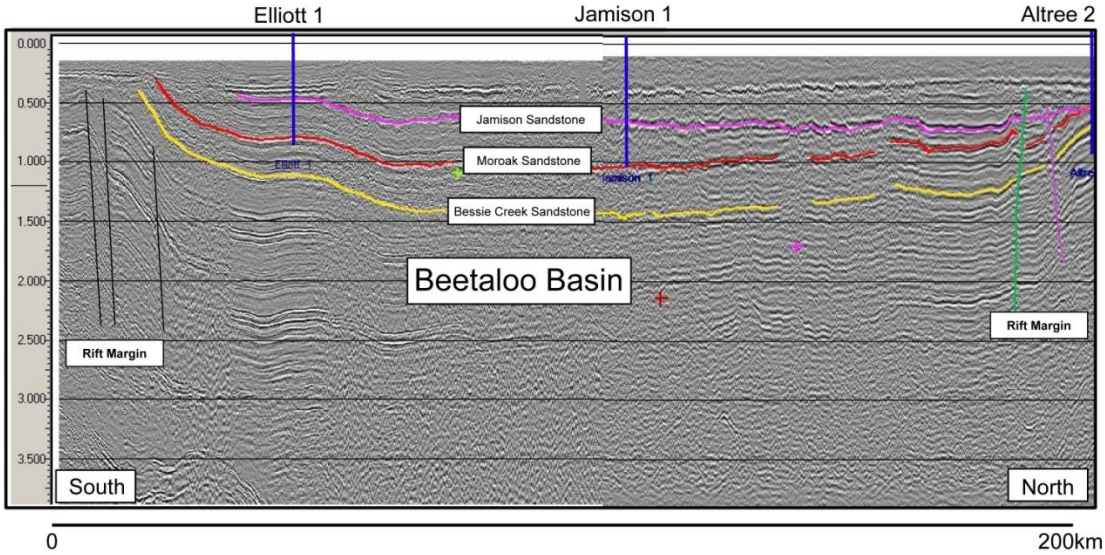

Figure 15: North - south trending 2-D seismic line 103 transecting the Beetaloo Basin. Location of seismic line 103 in Fig. 12, formations labelled; Bessie Creek Sandstone = yellow line, Moroak Sandstone = red line, Jamison Sandstone = pink line, drillholes indicated by blue line and labelled; Elliott 1, Jamison 1, Altree 2, rift margins identified to the south and north. (Redrafted from Silverman and Ahlbrandt, 2011).

CONCLUSIONS

Depositional age constraints of the Maiwok Sub-group in the Beetaloo Basin were determined primarily from detrital zircon geochronology. The Bessie Creek Sandstone formation was deposited between 1386 ± 13 Ma (2σ error) and 1324 ± 8 Ma (2σ error). The Moroak Sandstone formation was deposited after to 1375 ± 15 Ma (2σ error). The

Bukalorkmi Sandstone formation was deposited after to 1194 ± 25 Ma (2σ error). The Jamison Sandstone formation was deposited between 959 ± 18 Ma (2σ error) and 513 ± 12 Ma (2σ error).

Temporal provenance variations are minimal between the Bessie Creek Sandstone and the Moroak Sandstone, but much larger between the Moroak Sandstone and the Jamison/Bukalorkmi Sandstone formations.

Older zircon were sourced from the north, northwest, and northeast of the Beetaloo Basin, while relatively younger zircon were sourced from the east, south and southeast of the Beetaloo Basin. Dominant provenance source terranes to the Bessie Creek Sandstone and the Moroak Sandstone were the Mount Isa Province and Arunta Region, while the Musgrave Province was the provenance source to the Bukalorkmi Sandstone and the Jamison Sandstone.

I have identified the three main groups of detrital zircon spectra based on their similarities, Group 1 was dominated by Bessie Creek Sandstone samples, Group 2 was dominated by Moroak Sandstone samples and Group 3 was dominated by Jamison Sandstone samples, but the groups are not restricted to stratigraphic formations, which highlight the temporal and regional provenance variations. Provenance sources differ from north and south of the Walton High, in the Beetaloo Basin. The Walton High defined boundary affects all Maiwok Sub-group sandstones, including exposed formations in the Urapunga Region, which have been under appreciated in previous studies.

Provenance data from the Bessie Creek Sandstone and the Moroak Sandstone do not support the orogenic flexure basin model for the Beetaloo Basin. Although I have less provenance data from the Bukalorkmi Sandstone and the Jamison Sandstone. From the

combination of provenance data and seismic data of the Beetaloo Basin, I have concluded that these formations were not deposited in an orogenic flexure basin.

ACKNOWLEDGMENTS

I am very grateful for the funding from Santos and Centre for Tectonics, Resources and Exploration and the Northern Territory Geological Survey (NTGS) for providing core samples, thank you for your support.

I would like to thank my supervisor Alan Collins for the opportunity to do the research on this project. I am grateful for the support and advice from Alan Collins, my co-supervisor Juraj Farkas and Bo Yang (PhD student).

I thank Alan Collins, Juraj Farkas, Bo Yang and Billy Giuliano (Honours student) for their help collecting drillcore samples.

I thank Bo Yang for co-authoring our Australian Earth Science Conference (AESC) poster, crushing drillcore, and collecting a significant amount of the provenance source data.

I thank Alan Collins and De Nicholls from Santos for their advice on the AESC poster and on which drillcore to sample.

From Santos I thank Brenton Schoemaker, David Lemon, Barbara Stummer for their help with drillcore well correlations.

I thank Carine Ward and Jony Schneider for helping crush drillcore.

From the NTGS I thank Belinda Smith for her advice and hylogger training, and Tim Munson for providing zircon data from Balmain 1 and the Urapunga Region.

From Adelaide Microscopy I thank Ben Wade and Aoife McFadden for their advice on CL imaging, LA-ICP-MS operations and advice on processing U-Pb data.

I am very thankful for the support from my family, especially Carine Ward, Mum, Dad and Catherine Turnbull.

REFERENCES

ABBOTT, S. T. & SWEET, I. P. 2000. Tectonic control on third-order sequences in a siliciclastic ramp-style basin: An example from the Roper Superbasin (Mesoproterozoic), northern Australia. *Australian Journal of Earth Sciences* **47(3)**, 637-657.

ABBOTT, S. T., SWEET, I. P., PLUMB, K. A., YOUNG, D. N., CUTOVINOS, A., FERENCZI, P. A. & PIETSCH, B. A. 2001. Roper Region: Urapunga and Roper River Special, Northern Territory (Second Edition). 1:250 000 geological map series explanatory notes, SD 53-10, 11. Northern Territory Geological Survey and Geoscience Australia (National Geoscience Mapping Accord).

AHMAD, M. & MUNSON, T. J. 2013. Northern Territory Geological Survey, Geology and mineral resources of the Northern Territory, Special Publication 5. Northern Territory Geological Survey.

AHMAD, M. & SCRIMGEOUR, I. R. 2013. Chapter 2: Geological framework: in Ahmad M and Munson TJ (compilers). *'Geology and mineral resources of the Northern Territory'. Northern Territory Geological Survey, Special Publicatio*n 5.

AMATO, J. M., BOULLION, A. O., SERNA, A. M., SANDERS, A. E., FARMER, G. L., GEHRELS, G. E., & WOODEN, J. L. 2008. Evolution of the Mazatzal province and the timing of the Mazatzal orogeny: Insights from U-Pb geochronology and geochemistry of igneous and metasedimentary rocks in southern New Mexico. *Geological Society of America Bulletin* **120(3-4)**, 328-346.

BARTH, A. P., WOODEN, J. L., COLEMAN, D. S. & FANNING, C. M. 2000. Geochronology of the Proterozoic basement of south western most North America, and the origin and evolution of the Mojave crustal province. *Tectonics* **19(4)**, 616-629.

BARTH, A. P., WOODEN, J. L., COLEMAN, D. S. & VOGEL, M. B. 2009. Assembling and disassembling California: A zircon and monazite geochronologic framework for Proterozoic crustal evolution in southern California. *The Journal of Geology* **117(3)**, 221-239.

BETTS, P. G. & GILES, D. 2006. The 1800–1100 Ma tectonic evolution of Australia. *Precambrian Research* **144(1–2)**, 92–125.

BETTS, PG, ARMIT, RJ, & AILLERES, L. 2015. Potential-field interpretation mapping of the greater McArthur Basin. PGN Geoscience Report 15/2014. Geophysical and structural interpretation of the greater McArthur Basin. Northern Territory Geological Survey, Digital Information Package DIP 015.

BEYER, E. E., HOLLIS, J. A., WHELAN, J. A., GLASS, L. M., DONNELLAN, N., YAXLEY, G., ARMSTRONG, R., ALLEN, C. & SCHERSTÉN, A., 2013. Summary of results. NTGS laser ablation ICPMS and SHRIMP U-Pb, Hf and O geochronology project: Pine Creek Orogen, Arunta Region, Georgina Basin and McArthur Basin, July 2008–May 2011. *Northern Territory Geological Survey, Record* 2012-007.

BEYER, E. E., ALLEN, C. M., ARMSTRONG, R. & WOODHEAD, J. D. 2015. Summary of results. NTGS laser ablation ICPMS U-Pb and Hf geochronology project: selected samples from NAPPERBY 1:250 000 mapsheet area, Arunta Region, July 2010–January 2012. *Northern Territory Geological Survey, Record* 2015-009.

BEYER, E. E., DONNELLAN, N., MEFFRE, S. & THOMPSON, J. M. 2016. Summary of results. NTGS laser ablation ICP-MS in situ zircon and baddeleyite geochronology project: Mount Peake Gabbro, Arunta Region. *Northern Territory Geological Survey, Record* 2016-002.

BLEWETT, R. S., BLACK, L. P., SUN, S. S., KNUTSON, J., HUTTON, L. J. & BAIN, J. H. C. 1998. "U-Pb zircon and Sm-Nd geochronology of the Mesoproterozoic of North Queensland: implications for a Rodinian connection with the Belt supergroup of North America." *Precambrian Research* **89**. 101-127.

BODORKOS, S., BEYER, E. E., EDGOOSE, C. J., WHELAN, J. A., WEBB, G., VANDENBERG, L. C. & HALLETT, L. 2013. Summary of results. Joint NTGS–GA geochronology project: Central and eastern Arunta Region, January 2008 – June 2011. *Northern Territory Geological Survey, Record* 2013-003.

BURRETT, C. & BERRY, R. F. 2000. Proterozoic Australia-western United States (AUSWUS) fit between Laurentia and Australia. *Geology* **28**, 103-106.

CARSON, C. J., CLAOUÉ-LONG, J., STERN, R., CLOSE, D. F., SCRIMGEOUR, I. R. & GLASS, L. M. 2009. Summary of results. Joint NTGS-GA geochronology project: Central and eastern Arunta Region and Pine Creek Orogen, July 2006–May 2007. *Northern Territory Geological Survey, Record* 2009-001.

CHEW, D. M., PETRUS, J. A. & KAMBER, B. S. 2014. U–Pb LA–ICPMS dating using accessory mineral standards with variable common Pb. *Chemical Geology* **363**, 185-199.

CLOSE, D. 2016. Integrated geoscience projects through the CORE initiative. *Northern Territory 'Annual Geoscience exploration Seminar (AGES 2016) Record of abstracts'*. Northern Territory Geological Survey, Record 2016, 91-94.

CLOSE, D. I., BARUCH, E. T., ALTMANN, C. M., COTE, A. J., MOHINUDEEN, F. M., RICHARDS, B. & STONIER, S. 2016. Unconventional gas potential in Proterozoic source rocks: Exploring the Beetaloo Sub-basin. *Northern Territory 'Annual Geoscience exploration Seminar (AGES 2016) Record of abstracts'*. Northern Territory Geological Survey, Record 2016, 91-94.

COLLINS, A. S., PATRANABIS-DEB, S., ALEXANDER, E., BERTRAM, C. N., FALSTER, G. M., GORE, R. J., MACKINTOSH, J., DHANG, P. C., SAHA, D., PAYNE, J. L., JOURDAN, F., BACKÉ, G., HALVERSON, G. P. & WADE, B. P. 2015. Detrital mineral age, radiogenic isotopic stratigraphy and tectonic significance of the Cuddapah Basin, India. *Gondwana Research.* **28**, 1294-1309.

COX, G. M., JARRETT, A., EDWARDS, D., CROCKFORD, P. W., HALVERSON, G. P., COLLINS, A. S., POIRIER, A. & LI, Z.-X. 2016. Basin redox and primary productivity within the Mesoproterozoic Roper Seaway. *Chemical Geology* **440**, 101-114.

CRAIG, J., BIFFI, U., GALIMBERTI, R. F., GHORI, K. A. R., GORTER, J. D., HAKHOO, N., HERON, D. P. L. THUROW, J. & VECOLI, M. 2013. The palaeobiology and geochemistry of Precambrian hydrocarbon source rocks. *Marine and Petroleum Geology* **40**, 1-47.

CROSS, A. J., CLAOUÉ-LONG, J. C., SCRIMGEOUR, I. R., CLOSE, D. F. & EDGOOSE, C. J. 2005. Summary of results. Joint NTGS-GA geochronology project: southern Arunta Region. *Northern Territory Geological Survey, Record* 2004-003.

CROSS, A. J., CLAOUÉ-LONG, J. C., SCRIMGEOUR, I. R., CRISPE, A. & DONNELLAN, N. 2005b. Summary of results. Joint NTGS-GA geochronology project: northern Arunta and Tanami regions, 2000–2003. *Northern Territory Geological Survey, Record* 2005-003.

CROSS, A. J., CLAOUÉ-LONG, J. C., SCRIMGEOUR, I. R., AHMAD, M. & KRUSE, P. D. 2005c. Summary of results. Joint NTGS-GA geochronology project: Rum Jungle, basement to southern Georgina Basin and eastern Arunta Region 2001–2003. *Northern Territory Geological Survey, Record* 2005-006.

CROSS, A. J., PURDY, D. J., BULTITUDE, R. J., BROWN, D. D. & CARR, P. A., 2015. Summary of results. Joint GSQ–GA geochronology project: Thomson Orogen, New England Orogen, Mossman Orogen and Mount Isa region, 2011–2013. *Queensland Geological Record* 2016/03.

FARMER, G. L., BOWRING, S. A., MATZEL, J., MALDONADO, G. E., FEDO, C. & WODDEN, J. 2005. Paleoproterozoic Mojave province in the northwestern Mexico? Isotopic and U-Pb zircon geochronologic studies of Precambrian and Cambrian crystalline and sedimentary rocks, Caborca, Sonora. *Geological Society of America Special Paper* **393**, 183-198.

GHORI, K. A. R., CRAIG, J., THUSU, B., LUNING, S., & GEIGER, M. 2009. Global Infracambrian petroleum systems: a review. *Geological Society, London, Special Publications* **326(1)**, 109-136.

GIBSON, G. M., HENSON, P. A., NEUMAN, N. L., SOUTHGATE, P. N. & HUTTON, L. J. 2012. Paleoproterozoic-earliest Mesoproterozoic basin evolution in the Mount Isa region, northern Australia and implications for reconstructions of Nuna and Rodinia Supercontinents. *In*: Scott K. M. & Jell P. A. eds., *Ottawa, ON: Canada: International Union of Geological Sciences (IUGS)* Vol. 35, pp. 131-140.

GORTER, J. D. & GREY, K. 2012. Middle Proterozoic biostratigraphy and log correlations of the Kyalla and Chambers River Formations Beetaloo Sub-basin, Northern Territory, Australia. *Central Australian Basins Symposium (CABS) III. Poster. Petroleum Exploration Society of Australia.*

HALPIN, J. A., JENSEN, T., MCGOLDRICK, P., MEFFRE, S., BERRY, R. F., EVERARD, J. L., CALVER, C. R., THOMPSON, J., GOEMANN, K. & WHITTAKER, J. M. 2014. Authigenic monazite and detrital zircon dating from the Proterozoic Rocky Cape Group, Tasmania: Links to the Belt-Purcell Supergroup, North America. *Precambrian Research* **250**, 50-67.

HANLEY, L. M. & WINGATE, M. T. D. 2000. SHRIMP zircon age for an Early Cambrian dolerite dyke: am intrusive phase of the Antrim Plateau Volcanics of northern Australia. *Australian Journal of Earth Sciences* **47(6)** 1029-1040

HOSKIN, P. W. O. & BLACK, L. P. 2000. Metamorphic zircon formation by solid-state recrystallization of protolith igneous zircon. *Journal of metamorphic Geology* **18(4)**, 423-439.

HOLLIS, J.A., BEYER, E. E., WHELAN, J. A., KEMP, A. I. S., SCHERSTÉN, A. & GREIG, A. 2010. Summary of results. NTGS laser U-Pb and Hf geochronology project: Pine Creek Orogen, Murphy Inlier, McArthur Basin and Arunta Region, July 2007–June 2008. *Northern Territory Geological Survey, Record* 2010-001.

HOLLIS, J. A., CARSON, C. J., GLASS, L. M., KOSITCIN, N., SCHERSTÉN, A., WORDEN, K. E., ARMSTRONG, R. A., YAXLEY, G. M. & KEMP, A. I. S. 2014. Detrital zircon U–Pb–Hf and O isotope character of the Cahill Formation and Nourlangie Schist, Pine Creek Orogen: Implications for the tectonic correlation and evolution of the North Australian Craton. *Precambrian Research* **246**, 35-53.

JACKSON, M. J., POWELL, T. G., SUMMONS, R. E. & SWEET, I. P. 1986. Hydrocarbon shows and petroleum source rocks in sediments as old as 1.7 x 10^9 years. *Nature* **322(6081)**, 727–729.

JACKSON, M. J., SWEET, I. P., PAGE, R. W. & BRADSHAW, B. E., 1999. The South Nicholson and Roper Groups: Evidence for the early Mesoproterozoic Roper Superbasin. *In*: Bradshaw B. E. & Scott D. L. eds. *Integrated basin analysis of the Isa Superbasin using seismic, well-log and geopotential data: an evaluation of the economic potential of the northern Lawn Hill Platform. Australian Geological Survey Organisation Record* 1999/19 (CD-ROM), pp 36-45.

JACKSON, M. J. & SOUTHGATE, P. N. 2000. Evolution of three unconformity-bounded sandy carbonate successions in the McArthur River region of northern Australia: the Lawn, Wide and Doom Supersequences in a proximal part of the Isa Basin. *In*: Cockbain A. E. ed. *Carpentaria-Mt Isa Zinc Belt: basement framework, chronostratigraphy and geodynamic evolution of Proterozoic successions (thematic issue). Australian Journal of Earth Sciences* 47, pp 625-635.

JACKSON, S. E., PEARSON, N. J., GRIFFIN, W. L. & BELOUSOVA, E. A. 2004. The application of laser ablation--inductively coupled plasma mass spectrometry to in situ U-Pb zircon geochronology. *Chemical Geology* **211**, 47-69.

JAVAUX, E. J., KNOLL, A. H., & WALTER, M. R. 2004. TEM evidence for eukaryotic diversity in mid-Proterozoic oceans. *Geobiology* **2(3)**, 121-132.

KOSITCIN, N., CHAMPION, D. C. & HUSTON, D. L. 2009. Geodynamic Synthesis of the North Queensland Region and Implications for Metallogeny. *Geoscience Australia Record* 2009/30, pp 196.

KOSITCIN, N., CARSON, C. J., HOLLIS, J. A., GLASS, L. M., CLOSE, D. F., WHELAN, J. A., WEBB, G. & DONNELLAN, N. 2013. Summary of results. Joint NTGS–GA geochronology project: Arunta Region, Davenport Province and Pine Creek Orogen July 2009 – June 2011. *Northern Territory Geological Survey, Record* 2012-008.

KOSITCIN, N., BEYER, E. E., WHELAN, J. A., CLOSE, D. F., HALLETT, L. & DUNKLEY, D. J. 2013b. Summary of results. Joint NTGS–GA geochronology project: Arunta Region, Ngalia Basin, Tanami Region and Murphy Province, July 2011–June 2012. *Northern Territory Geological Survey, Record* 2013-004.

KOSITCIN, N., WHELAN, J. A., HALLETT, L. & BEYER, E. E., 2014. Summary of results. Joint NTGS–GA geochronology project: Amadeus Basin, Arunta Region and Murphy Province, July 2012–June 2013. *Northern Territory Geological Survey, Record* 2014-005.

KOSITCIN, N., BEYER, E. E. & WHELAN, J. A., 2014b. Summary of results. Joint NTGS–GA SHRIMP geochronology project: Arunta Region, July 2013–June 2014. *Northern Territory Geological Survey, Record* 2014‑008.

KOSITCIN, N., KRAUS, S. & WHELAN, J. A. 2015. Summary of results. Joint NTGS–GA SHRIMP geochronology project: Arnhem Province, July 2014–June 2015. *Northern Territory Geological Survey, Record* 2015-010

KOSITCIN, N., RENO, B. L. & WHELAN, J. A. 2015b. Summary of results. Joint NTGS–GA geochronology project: Arunta Region, July 2014–June 2015. *Northern Territory Geological Survey, Record* 2015-007.

LEDLIE, I. & WESTE, G. 1989. Walton 2, Section 2 – Geological Data Summary. Pacific Oil & Gas Pty Limited, 17-27.

LI, Z.-X. & EVANS, D. A. D. 2011. Late Neoproterozoic 40° intraplate rotation within Australia allows for a tighter-fitting and longer-lasting Rodinia. *Geological Society of America* **39(1),** 39–42.

LUDWIG, K. R. 2003. User's Manual for Isoplot/Ex, Version 3.00, A Geochronological Toolkit for Microsoft Excel. Berkeley: Berkeley Geochronology Center Special Publication.

MACLEAN, J. S. 2007. Detrital-zircon geochronologic provenance analyses that test and expand the East Siberia-West Laurentia Rodinia reconstruction. *These, Dissertations, Professional Papers.* Paper 1216

MAHON, R. C., DEHLER, C. M., LINK, P. K., KARLSTROM, K. E. & GEHRELS, G. E. 2014. Detrital zircon provenance and paleogeography of the Pahrump Group and overlying strata, Death Valley, California. *Precambrian Research* **251**, 102-117.

MEDIG, K. P. R., THORKELSON, D. J., DAVIS, W. J., RAINBIRD, R. H., GIBSON, H. D., TURNER, E. C. & MARSHALL, D. D. 2014. Pinning northeastern Australia to northwestern Laurentia in the Mesoproterozoic. *Precambrian Research* **249**, 88-99.

MUNSON, T. J. 2016. Sedimentary characterisation of the Wilton package, greater McArthur Basin. Northern Territory. *'Annual Geoscience exploration Seminar (AGES 2016) Record of abstracts'.* Northern Territory Geological Survey, Record 2016, 84-89.

MUNSON, T. J., THOMPSON, J. M., ZHUKOVA, I., MEFFRE, S., BEYER, E. E. & WHELAN, J. A. in prep. Summary of results. NTGS laser ablation ICPMS geochronology project: Roper Group (McArthur Basin), Renner Group (Tomkinson Province), Tijunna Group (Birrindudu Basin). Northern Territory Geological Survey, Record.

NEMCHIN, A. A. & CAWOOD, P. A. 2005. Discordance of the U-Pb system in detrital zircons: Implication for provenance studies of sedimentary rocks. *Sedimentary Geology*, **182(1-4)**, 143-162.

NEUMANN, N. L., GIBSON, G. M. & SOUTHGATE, P. N. 2009. New SHRIMP age constraints on the timing and duration of magmatism and sedimentation in the Mary Kathleen Fold Belt, Mt Isa Inlier, Australia. *Australian Journal of Earth Sciences* **56(7)**, 965-983.

NEUMANN, N. L., SOUTHGATE, P. N., GIBSON, G. M. & MCINTYRE, A. 2006. New SHRIMP geochronology for the Western Fold Belt of the Mt Isa Inlier: developing a 1800 – 1650 Ma event framework. *Australian Journal of Earth Sciences* **53(6)**, 1023-1039.

PAGE, R. W. & SUN, S.-S. 1998. Aspects of geochronology and crustal evolution in the Eastern Fold Belt, Mt Isa Inlier. *Australian Journal of Earth Sciences* **45(3)**, 343-361.

PAYNE, J. L., FERRIS, G., BAROVICH, K. M. & HAND, M. 2010. Pitfalls of classifying ancient magmatic suites with tectonic discrimination diagrams: An example from the Paleoproterozoic Tunkillia Suite, southern Australia. *Precambrian Research* **177(3-4)**, 227-240.

PLUMB, K. A. & WELLMAN, P. 1987. McArthur Basin, Northern Territory: mapping of deep troughs using gravity and magnetic anomalies. *BMR Journal of Australian Geology & Geophysics* **10**, 243-251.

RÄMÖ, O. T., MCLEMORE, V. T., HAMILTON, M. A., KOSUNEN, P. J., HEIZLER, M. & HAAPALA, I. 2003. Intermittent 1630–1220 Ma magmatism in central Mazatzal Province: New geochronologic piercing points and some tectonic implications. *Geology* **31(4)**, 335-338.

RAWLINGS, D.J. 1999. Stratigraphic resolution of a multiphase intracratonic basin system: The McArthur Basin, northern Australia. *Australian Journal of Earth Sciences* **46(5)**, 703-723.

REVIE, D. 2016. From the back of the shed to the forefront of exploration: what the NTGS core store is revealing about the Roper Group shales of the greater McArthur Basin. *'Annual Geoscience Exploration Seminar (AGES) Proceedings, Alice Springs, Northern Territory 15–16 March 2016'*. Northern Territory Geological Survey, Darwin.

SCOTT, D. L., BRADSHAW, B. E. & TARLOWSKI, C. Z. 1998. The tectonostratigraphic history of the Proterozoic Northern Lawn Hill Platform, Australia: an integrated intracontinental basin analysis. *Tectonophysics* **300**, 329–358.

SILVERMAN, M. R., LANDON, S. M., LEAVER, J. S., MATHER, T. J. & BERG, E. 2005. No fuel like an old fuel: Proterozoic oil and gas potential in the Beetaloo Basin, Northern Territory, Australia. *In*: Munson T. J. & Ambrose G. T. eds. '*Proceedings of the Central Australian Basins Symposium (CABS), Alice Springs, Northern Territory, 16–18 August, 2005'.* Northern Territory Geological Survey, Special Publication 2, pp. 205–215.

SILVERMAN, M. & AHLBRANDT, T. 2011. Mesoproterozoic Unconventional Plays in the Beetaloo Basin, Australia: The World's Oldest Petroleum Systems. *AAPP International Conference and Exhibition, Calgary, Alberta, 2011,* 1-41.

SLAMA, J., KOSLER, J., CONDON, D. J., CROWLEY, J. L., GERDES, A., HANCHAR, J. M., HORSTWOOD, M. S. A., MORRIS, G. A., NASDALA, L., NORBERG, N., SCHALTEGGER, U., SCHOENE, B., TUBRETT, M. N. & WHITEHOUSE, M. J. 2008. Plesovic zircon-A new natural reference material for U-Pb and Hf isotopic microanalysis. *Chemical Geology* **249**, 1-35.

SMITH, B. R. 2015.Hylogger drillhole report for BMR Urapunga 5, McArthur Basin, Northern Territory. *Northern Territory Geological Survey, Hylogger Data Package* 0042.

SPENCER, C. J., KIRKLAND, C. L. & TAYLOR, R. J. M. 2016. Strategies towards statistically robust interpretations of in situ U–Pb zircon geochronology. *Geoscience Frontiers* **7(4)**, 581-589.

TORKINGTON, J. & LANIGAN, K. 1991. Well Completion Report EP 19 – Sever-1, Appendix 6, Geological Description. Pacific Oil & Gas Pty Limited, Report No:304297, 48-67.

TRAVES, D. M. 1955. The geology of the Ord-Victoria region, northern Australia. *Bureau of Mineral Resources, Australia, Bulletin* **27**

VERMEESCH, P. 2013. Multi-sample comparison of detrital age distributions. *Chemical Geology* **341**, 140-146.

WADE, B. P. 2006. Unravelling the tectonic framework of the Musgrave Province, central Australia. PhD Thesis. University of Adelaide.

WESTE, G., TORKINGTON, J. & CHIUPKA, J. 1988. Altree 2, Well Summary. Pacific Oil & Gas Pty Limited, 1-4.

WORDEN, K. E., CLAOUÉ-LONG, J. C., SCRMGEOUR, I. R. & DOYLE, N. 2006. Summary of results. Joint NTGS-GA geochronology project: Pine Creek Orogen and Arunta Region, January–June 2004. *Northern Territory Geological Survey, Record* 2006-005.

WORDEN, K. E., CLAOUÉ-LONG, J. C. & SCRIMGEOUR, I. R. 2006b. Summary of results. Joint NTGS-GA geochronology project: Pine Creek Orogen, Tanami Region, Arunta Region and Amadeus Basin, July–December 2004. *Northern Territory Geological Survey, Record* 2006-006.

WORDEN, K. E., CARSOU, C. J., CLOSE, D. F., DONNELLAN, N. & SCRIMGEOUR, I. R. 2008. Summary of results. Joint NTGS-GA geochronology project: Tanami Region, Arunta Region, Pine Creek Orogen and Halls Creek January 2005–March 2007. *Northern Territory Geological Survey, Record* 2008-003.

YANG, B. et al. in prep. Spatial and Temporal Provenance Analysis of the Upper Roper Group, Beetaloo Basin, North Australia.

APPENDIX A: ALL DATA CONCORDIA PLOTS

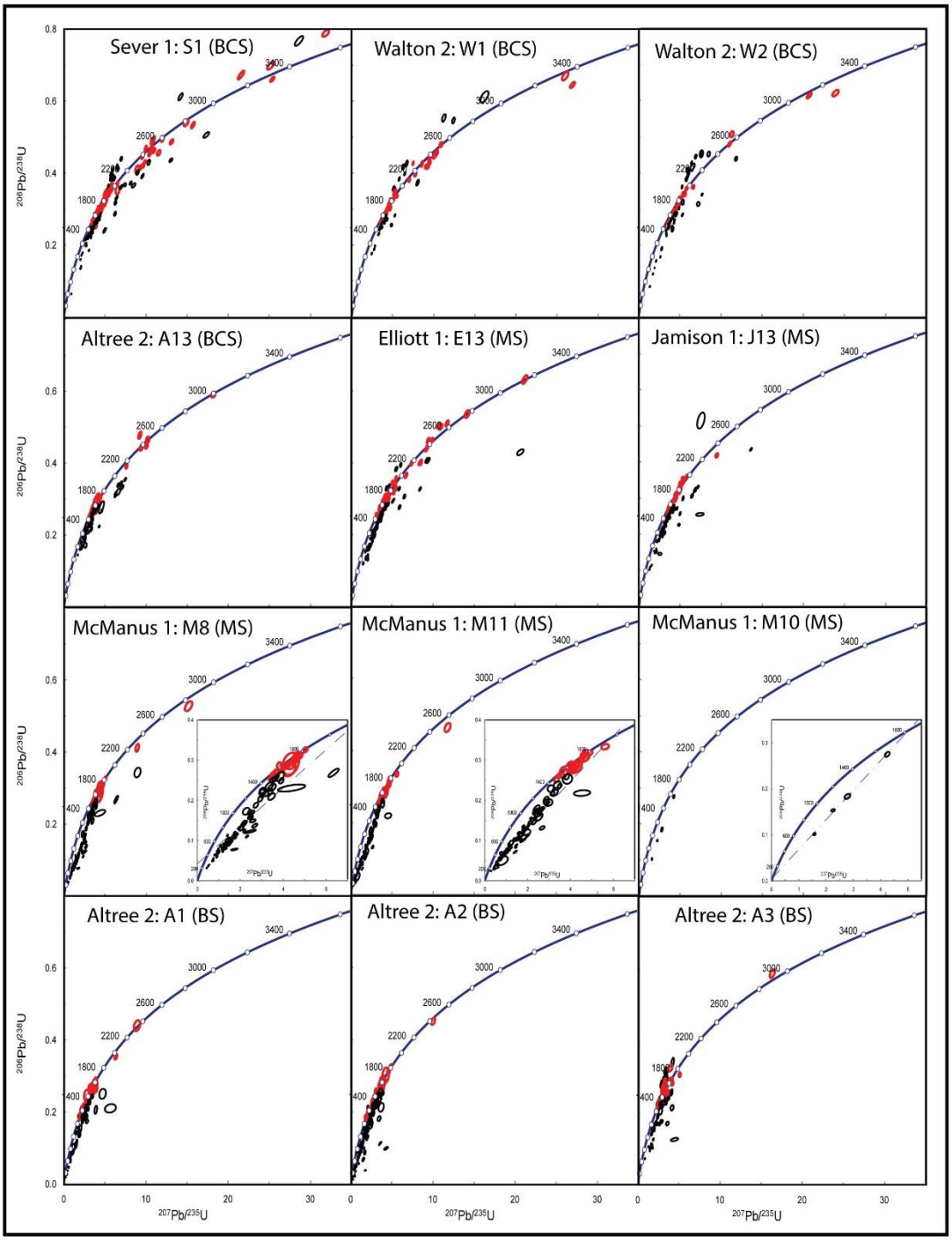

Figure 16: All U–Pb data concordia plots, of 12 core samples, taken from Beetaloo Basin. Sample locations are illustrated in Fig .1 and located in Table 1. Samples are labelled (core hole, samples number, formation), $^{206}Pb/^{238}U$ v $^{207}Pb/^{235}U$ plots, n = number of concordant analyses. Data point error ellipses are 2 standard deviations. Data coloured based on concordance; black = <90%, red = >90%.

APPENDIX B: ZIRCON DATA

Table 3: U-Pb >90% concordant zircon data. Note that black = Neoproterozoic, blue = Mesoproterozoic, red = Palaeoproterozoic, purple = Archaean.

S1 - Sever 1 - BCS										
	Final 207_235	Final 207_235 _Int2SE	Final 206_238	Final 206_238 _Int2SE	Error Correlation _6_38v7_35	Conc (%)	FinalAge 206_238	FinalAge 206_238 _Int2SE	FinalAge 207_206	FinalAge 207_206 _Int2SE
1	2.907	0.028	0.2399	0.0025	0.70549	102	1386	13	1354	14
2	3.072	0.043	0.2345	0.003	0.5261	90	1358	16	1505	25
3	3.488	0.078	0.2681	0.0043	0.32251	101	1532	22	1513	46
4	3.683	0.032	0.2798	0.0023	0.56687	104	1590	12	1527	15
5	3.396	0.05	0.2553	0.0028	0.5929	95	1465	15	1535	24
6	3.774	0.079	0.2837	0.005	0.31318	104	1608	25	1542	39
7	3.667	0.062	0.2718	0.0038	0.35014	100	1549	19	1550	34
8	3.277	0.038	0.242	0.0024	0.69783	90	1397	13	1557	15
9	3.4	0.045	0.256	0.0029	0.57958	94	1469	15	1562	23
10	3.847	0.053	0.2843	0.0032	0.32653	102	1612	16	1578	28
11	3.995	0.08	0.2906	0.0053	0.34802	103	1642	26	1596	44
12	3.43	0.072	0.2505	0.0035	0.32634	90	1440	18	1598	38
13	4.199	0.074	0.3018	0.0052	0.33714	104	1701	25	1643	35
14	3.62	0.13	0.2645	0.0061	0.26286	91	1510	31	1651	69
15	4.359	0.075	0.3029	0.0049	0.52701	101	1708	25	1688	29
16	3.895	0.052	0.2724	0.0039	0.44927	92	1552	20	1692	27
17	4.343	0.055	0.2994	0.0041	0.59003	100	1689	20	1695	22
18	4.426	0.065	0.3039	0.0052	0.69256	101	1711	25	1695	22
19	3.899	0.049	0.2706	0.0031	0.47764	91	1543	16	1699	23
20	4.057	0.065	0.2807	0.0038	0.33647	94	1596	19	1700	30

21	4.383	0.087	0.2962	0.0039	0.30307	98	1672	19	1702	38
22	4.013	0.048	0.2807	0.0029	0.58819	93	1594	15	1707	19
23	4.185	0.065	0.2926	0.0041	0.4413	97	1657	21	1708	27
24	4.547	0.058	0.3138	0.0032	0.40621	103	1759	16	1713	25
25	4.015	0.063	0.2776	0.0036	0.39056	92	1578	18	1713	27
26	4.338	0.085	0.2944	0.0047	0.54143	97	1662	23	1714	32
27	4.117	0.058	0.2841	0.0036	0.48479	94	1611	18	1716	27
28	4.177	0.063	0.2834	0.0037	0.53249	93	1608	19	1723	26
29	3.963	0.055	0.2723	0.003	0.4629	90	1552	15	1724	23
30	4.242	0.072	0.2921	0.0039	0.55598	96	1651	19	1725	26
31	4.483	0.075	0.3088	0.004	0.40035	100	1733	20	1728	29
32	4.437	0.055	0.2998	0.0038	0.38887	97	1690	19	1737	25
33	4.03	0.056	0.2753	0.0035	0.55884	90	1570	17	1738	23
34	5.05	0.11	0.3439	0.006	0.64337	109	1903	29	1739	31
35	4.309	0.089	0.2945	0.0047	0.38496	96	1666	23	1740	38
36	4.201	0.065	0.2878	0.0042	0.21077	94	1630	21	1740	39
37	4.986	0.088	0.3386	0.0051	0.55572	108	1878	25	1741	30
38	4.235	0.05	0.2887	0.0033	0.51825	94	1634	17	1743	22
39	4.752	0.081	0.3226	0.0049	0.51253	103	1804	24	1744	29
40	4.346	0.06	0.2977	0.0037	0.27691	96	1679	18	1754	29
41	4.6	0.11	0.3117	0.0064	0.75108	99	1747	32	1759	28
42	4.606	0.06	0.3123	0.0034	0.50399	99	1751	17	1760	21
43	4.145	0.079	0.2799	0.0039	0.57461	90	1592	19	1761	28
44	4.493	0.082	0.3007	0.0057	0.6072	96	1693	28	1763	28
45	4.749	0.071	0.3185	0.0038	0.60753	101	1782	19	1766	21
46	5.162	0.049	0.3433	0.0031	0.67042	107	1902	15	1779	14
47	4.592	0.057	0.3013	0.0041	0.43082	95	1697	20	1790	25
48	4.68	0.13	0.3046	0.0049	0.29198	95	1713	24	1794	50
49	5.146	0.079	0.3333	0.0048	0.57862	103	1855	23	1802	24

50	4.471	0.058	0.2946	0.0032	0.51059	92	1665	16	1809	22
51	4.901	0.099	0.3209	0.0061	0.83331	99	1800	29	1810	21
52	4.662	0.064	0.3044	0.0037	0.46727	94	1712	18	1817	26
53	5.449	0.073	0.3509	0.0045	0.55688	107	1939	22	1819	24
54	4.605	0.084	0.2963	0.0043	0.45446	92	1672	22	1827	31
55	4.559	0.055	0.2946	0.0031	0.70342	91	1666	15	1838	16
56	4.688	0.059	0.3031	0.0031	0.35743	93	1707	15	1843	24
57	4.552	0.049	0.293	0.0028	0.57736	90	1656	14	1845	18
58	4.484	0.055	0.2925	0.0034	0.54661	90	1653	17	1845	21
59	4.839	0.073	0.3109	0.0038	0.42924	94	1744	18	1852	27
60	5.181	0.077	0.3227	0.0049	0.62738	97	1805	24	1858	22
61	5.174	0.098	0.3295	0.0049	0.51805	98	1835	24	1865	26
62	5.812	0.085	0.3682	0.0047	0.64535	108	2020	22	1869	20
63	5.101	0.062	0.3215	0.0033	0.58375	96	1798	16	1875	19
64	4.984	0.07	0.312	0.0033	0.36082	93	1752	16	1876	25
65	5.466	0.07	0.3386	0.004	0.66812	99	1879	19	1901	18
66	5.536	0.09	0.3426	0.0057	0.3699	100	1898	28	1902	33
67	5.754	0.093	0.3506	0.0057	0.65328	101	1938	28	1912	22
68	5.847	0.091	0.355	0.0054	0.53052	101	1959	25	1944	26
69	6.544	0.09	0.3708	0.0043	0.43124	99	2032	20	2060	25
70	6.53	0.19	0.3516	0.0092	0.20127	90	1941	44	2157	60
71	9.99	0.11	0.4681	0.0061	0.56426	103	2474	27	2393	18
72	9.6	0.12	0.4458	0.0053	0.62811	98	2375	24	2423	18
73	8.93	0.18	0.4097	0.0088	0.39263	91	2212	40	2438	38
74	10.95	0.11	0.4943	0.0054	0.69633	105	2588	23	2464	15
75	10.79	0.18	0.4879	0.008	0.43805	104	2565	34	2470	28
76	9.3	0.13	0.4146	0.0051	0.4993	90	2234	23	2490	22
77	9.905	0.093	0.4312	0.0037	0.54974	92	2310	16	2505	15
78	10.68	0.12	0.4701	0.0045	0.62624	99	2488	20	2506	16

79	9.64	0.13	0.4204	0.005	0.55012	90	2261	23	2516	20
80	10.46	0.16	0.4552	0.0074	0.67146	95	2418	33	2539	22
81	10.98	0.13	0.4624	0.0061	0.67972	96	2448	27	2541	16
82	12.02	0.14	0.4942	0.0065	0.58752	99	2586	28	2618	18
83	11.55	0.17	0.456	0.0059	0.53331	91	2421	26	2662	21
84	13.1	0.18	0.4863	0.0059	0.69507	91	2554	26	2797	16
85	14.89	0.24	0.5403	0.0081	0.54924	99	2789	34	2805	25
86	15.72	0.2	0.5329	0.0071	0.78628	94	2751	30	2936	14
87	21.58	0.31	0.672	0.01	0.8535	108	3312	40	3078	12
88	25.19	0.35	0.6986	0.0093	0.74008	105	3412	35	3240	15
89	25.36	0.21	0.6599	0.0057	0.78772	98	3266	22	3339	8.3
90	31.88	0.33	0.7883	0.0076	0.6099	109	3745	27	3443	13

W1 - Walton 2 – BCS

	Final 207_235	Final 207_235 _Int2SE	Final 206_238	Final 206_238 _Int2SE	Error Correlation _6_38v7_35	Conc (%)	FinalAge 206_238	FinalAge 206_238 _Int2SE	FinalAge 207_206	FinalAge 207_206 _Int2SE
1	3.526	0.049	0.2648	0.0032	0.40054	96	1515	16	1579	27
2	3.507	0.047	0.2576	0.0029	0.50851	91	1477	15	1621	24
3	4.003	0.053	0.2809	0.0035	0.5042	94	1595	17	1697	23
4	3.934	0.048	0.2744	0.0034	0.62974	90	1563	17	1728	18
5	4.272	0.049	0.2951	0.0027	0.55999	96	1667	13	1730	19
6	4.403	0.061	0.3026	0.0041	0.60658	98	1705	20	1735	22
7	4.103	0.094	0.2814	0.005	0.47661	92	1598	25	1735	37
8	4.289	0.06	0.2958	0.0032	0.63339	96	1670	16	1736	18
9	4.168	0.054	0.2871	0.0033	0.42256	94	1626	16	1738	25
10	4.314	0.054	0.2987	0.0032	0.40626	97	1686	16	1740	23
11	4.632	0.057	0.3187	0.0037	0.47226	102	1782	18	1741	22

12	4.325	0.061	0.2951	0.0037	0.61368	96	1668	19	1741	20
13	4.192	0.082	0.2871	0.005	0.44038	93	1626	25	1742	35
14	4.538	0.068	0.3123	0.0037	0.47421	100	1751	18	1747	25
15	4.073	0.061	0.2798	0.0033	0.73003	91	1590	17	1747	17
16	4.746	0.05	0.3257	0.0031	0.43281	104	1817	15	1748	18
17	4.111	0.048	0.2826	0.0027	0.37656	92	1604	13	1751	22
18	4.302	0.056	0.2969	0.0038	0.47109	95	1675	19	1754	26
19	4.189	0.055	0.2839	0.0034	0.53738	91	1610	17	1764	22
20	4.294	0.062	0.2897	0.0039	0.42374	93	1641	19	1770	27
21	4.189	0.075	0.2822	0.0042	0.63556	90	1604	21	1784	24
22	4.685	0.051	0.311	0.0028	0.41738	97	1745	14	1805	21
23	5.223	0.086	0.3467	0.0045	0.54845	106	1919	22	1808	24
24	5.229	0.084	0.3399	0.0054	0.56162	103	1885	26	1830	25
25	4.74	0.055	0.3125	0.0035	0.74688	96	1754	18	1833	15
26	4.898	0.054	0.3196	0.0033	0.64135	97	1787	16	1839	17
27	4.73	0.082	0.3029	0.0049	0.31035	93	1707	24	1840	36
28	4.712	0.09	0.3028	0.0057	0.46294	92	1704	28	1846	36
29	5.388	0.073	0.3496	0.0041	0.45796	104	1932	20	1853	25
30	4.755	0.05	0.3046	0.0034	0.65553	92	1715	17	1860	15
31	5.147	0.062	0.3253	0.0033	0.64263	96	1815	16	1898	16
32	5.528	0.066	0.3349	0.0035	0.46048	96	1862	17	1942	22
33	7.503	0.063	0.4271	0.0039	0.66647	110	2293	18	2081	13
34	7.049	0.081	0.3805	0.0041	0.50804	96	2078	19	2167	18
35	7.774	0.099	0.3958	0.0046	0.67142	94	2152	21	2281	16
36	8.58	0.11	0.4256	0.0063	0.65858	98	2288	28	2327	19
37	9.5	0.13	0.4423	0.0063	0.48597	98	2362	28	2420	24
38	9.1	0.1	0.4174	0.0046	0.41831	92	2250	21	2444	21
39	9.8	0.11	0.4501	0.0046	0.54376	98	2395	21	2454	17
40	9.49	0.14	0.4276	0.0064	0.58819	92	2293	29	2485	22

41	9.307	0.077	0.4161	0.004	0.40472	90	2243	18	2493	16
42	10.12	0.18	0.4478	0.0065	0.55722	95	2384	29	2498	27
43	10.35	0.16	0.4555	0.0068	0.54547	96	2421	30	2517	24
44	10.92	0.14	0.4788	0.0059	0.37965	99	2523	26	2539	25
45	26.01	0.3	0.6699	0.0096	0.64749	97	3304	37	3394	17
46	26.91	0.24	0.6451	0.0068	0.75258	92	3210	27	3505	11

W2 - Walton 2 - BCS

	Final 207_235	Final 207_235 _Int2SE	Final 206_238	Final 206_238 _Int2SE	Error Correlation _6_38v7_35	Conc (%)	FinalAge 206_238	FinalAge 206_238 _Int2SE	FinalAge 207_206	FinalAge 207_206 _Int2SE
1	3.255	0.052	0.2458	0.0027	0.50814	92	1416	14	1539	26
2	3.54	0.064	0.2599	0.0032	0.39544	93	1488	16	1598	32
3	3.973	0.043	0.2805	0.0025	0.49785	96	1594	13	1669	19
4	3.833	0.083	0.2682	0.0039	0.26768	90	1531	20	1705	42
5	4.287	0.054	0.2947	0.0035	0.59934	97	1665	17	1723	19
6	4.614	0.069	0.3123	0.0038	0.54939	101	1751	18	1739	22
7	4.284	0.063	0.2898	0.0033	0.4341	94	1642	17	1739	25
8	4.136	0.052	0.2826	0.0031	0.66878	92	1604	16	1745	18
9	4.212	0.064	0.2839	0.0029	0.42494	92	1611	15	1755	27
10	4.29	0.057	0.2876	0.0035	0.457	93	1631	18	1761	27
11	4.964	0.073	0.3292	0.0037	0.51862	104	1834	18	1768	24
12	4.453	0.061	0.295	0.0036	0.33197	94	1669	18	1777	27
13	4.901	0.07	0.321	0.0037	0.6166	100	1794	18	1798	20
14	4.531	0.059	0.2944	0.0032	0.49371	92	1664	16	1808	21
15	4.859	0.071	0.3192	0.0049	0.61778	99	1793	12	1809	24
16	4.744	0.068	0.3072	0.0039	0.35178	95	1728	19	1820	29
17	4.628	0.044	0.2973	0.0026	0.64122	91	1678	13	1843	14

18	5.049	0.071	0.3165	0.0036	0.19731	96	1772	18	1854	30
19	4.886	0.094	0.3101	0.0055	0.24135	94	1740	27	1856	42
20	5.312	0.053	0.3325	0.0029	0.5092	99	1850	14	1869	17
21	5.396	0.089	0.3395	0.0052	0.5357	99	1884	14	1906	28
22	5.807	0.085	0.3551	0.0045	0.53021	101	1957	21	1933	25
23	5.678	0.073	0.3391	0.0038	0.42884	95	1882	18	1972	22
24	6.657	0.09	0.3601	0.0039	0.43635	92	1984	18	2147	23
25	11.33	0.17	0.5064	0.0067	0.40552	107	2639	29	2464	26
26	11.06	0.16	0.479	0.0057	0.72601	100	2522	25	2532	17
27	20.72	0.25	0.6132	0.0066	0.76882	98	3082	27	3158	12
28	23.94	0.31	0.6207	0.0074	0.6387	93	3114	29	3351	17

A13 - Altree 2 - BCS

	Final 207_235	Final 207_235 _Int2SE	Final 206_238	Final 206_238 _Int2SE	Error Correlation _6_38v7_35	Conc (%)	FinalAge 206_238	FinalAge 206_238 _Int2SE	FinalAge 207_206	FinalAge 207_206 _Int2SE
1	3.071	0.069	0.2519	0.0041	0.45215	103	1447	21	1409	42
2	3.094	0.053	0.25	0.0036	0.40784	101	1440	18	1421	32
3	2.801	0.047	0.2223	0.0032	0.33422	90	1294	17	1433	36
4	3.065	0.052	0.2449	0.0038	0.49712	97	1411	20	1454	31
5	3.144	0.051	0.2516	0.0036	0.33462	99	1446	18	1466	31
6	3.04	0.1	0.2468	0.0055	0.38637	96	1421	29	1475	64
7	3.445	0.058	0.268	0.0034	0.36814	102	1530	17	1493	30
8	3.172	0.072	0.2557	0.0049	0.32646	98	1467	25	1498	49
9	3.272	0.065	0.2576	0.0045	0.47547	98	1479	23	1510	34
10	3.68	0.081	0.2843	0.0044	0.28865	107	1612	22	1511	41
11	3.574	0.055	0.2711	0.0033	0.23221	102	1546	17	1513	31

12	3.35	0.083	0.2622	0.0045	0.40331	99	1503	23	1519	47
13	3.586	0.05	0.273	0.0026	0.18714	102	1556	13	1524	29
14	3.563	0.074	0.2696	0.0046	0.2039	100	1538	23	1532	44
15	3.669	0.053	0.288	0.0032	0.48195	106	1631	16	1539	26
16	3.429	0.063	0.2557	0.0039	0.33849	95	1467	20	1539	34
17	3.291	0.055	0.2488	0.0036	0.19901	93	1431	19	1539	36
18	3.287	0.072	0.2446	0.004	0.41211	92	1412	21	1540	40
19	3.145	0.076	0.2475	0.0053	0.56071	92	1428	28	1547	37
20	3.566	0.071	0.271	0.004	0.16542	99	1545	21	1555	39
21	4.17	0.13	0.3065	0.0063	0.019275	109	1722	31	1575	67
22	3.45	0.19	0.267	0.011	0.51258	95	1522	56	1598	96
23	4.1	0.059	0.298	0.0039	0.45177	105	1680	19	1601	25
24	3.48	0.12	0.2631	0.0086	0.50697	94	1503	44	1606	65
25	3.708	0.05	0.2773	0.0047	0.41545	98	1577	24	1616	27
26	3.62	0.21	0.273	0.012	0.40096	95	1550	63	1636	81
27	4.212	0.067	0.3089	0.0053	0.57212	106	1734	26	1642	29
28	3.785	0.05	0.2701	0.0032	0.37446	94	1540	16	1645	26
29	3.705	0.073	0.2699	0.0046	0.47717	93	1539	23	1648	37
30	3.448	0.07	0.2606	0.0052	0.53199	90	1492	27	1654	37
31	3.653	0.055	0.2598	0.0032	0.54219	90	1489	16	1655	23
32	3.883	0.051	0.2754	0.0032	0.40156	94	1567	16	1663	24
33	4.336	0.065	0.3083	0.0041	0.49087	104	1732	20	1668	24
34	4.266	0.097	0.3062	0.0063	0.64325	102	1721	31	1692	35
35	4.338	0.066	0.3014	0.004	0.091459	100	1697	20	1692	29
36	3.947	0.077	0.2789	0.0039	0.42588	93	1588	20	1706	30
37	4.178	0.069	0.2937	0.005	0.40975	97	1659	25	1708	32
38	4.392	0.077	0.3035	0.004	0.26608	100	1711	19	1710	33
39	4.335	0.066	0.2975	0.004	0.53023	98	1680	19	1712	24
40	4.163	0.078	0.2935	0.0051	0.48849	96	1658	25	1725	33

41	4.411	0.099	0.3044	0.0055	0.28626	99	1714	27	1726	45
42	4.232	0.054	0.2895	0.0033	0.36859	95	1639	16	1730	23
43	4.266	0.079	0.2877	0.0042	0.50161	94	1631	21	1743	28
44	4.03	0.1	0.2879	0.0069	0.58239	93	1630	34	1759	44
45	4.304	0.076	0.2961	0.0045	0.52812	95	1671	22	1763	32
46	4.803	0.089	0.3208	0.0048	0.34469	101	1792	24	1780	36
47	4.499	0.072	0.3064	0.0046	0.52454	95	1722	23	1805	27
48	7.618	0.099	0.3917	0.0056	0.52445	95	2132	26	2255	21
49	9.25	0.15	0.4773	0.0086	0.60221	110	2514	37	2282	21
50	9.43	0.16	0.4437	0.0074	0.58106	98	2369	33	2422	27
51	10.19	0.17	0.464	0.0077	0.37776	99	2455	34	2475	28
52	10.04	0.12	0.4459	0.0048	0.50777	96	2378	21	2476	18
53	18.18	0.2	0.5904	0.0069	0.36472	100	2989	28	2987	18

E13 - Elliott 1 - MS

	Final 207_235	Final 207_235 _Int2SE	Final 206_238	Final 206_238 _Int2SE	Error Correlation _6_38v7_35	Conc (%)	FinalAge 206_238	FinalAge 206_238 _Int2SE	FinalAge 207_206	FinalAge 207_206 _Int2SE
1	3.095	0.045	0.2564	0.0033	0.73572	106	1470	17	1383	18
2	3.05	0.061	0.237	0.0038	0.37279	93	1371	20	1469	37
3	3.476	0.091	0.2639	0.0056	0.13807	98	1512	28	1550	57
4	3.195	0.059	0.2433	0.0039	0.48807	90	1403	20	1551	31
5	3.478	0.063	0.2656	0.004	0.52336	97	1517	20	1558	29
6	3.261	0.07	0.2483	0.0048	0.53294	92	1429	25	1558	35
7	3.521	0.072	0.2659	0.0045	0.59107	98	1522	23	1561	32
8	3.268	0.07	0.2477	0.0044	0.36323	91	1427	22	1561	44
9	3.647	0.058	0.2769	0.0041	0.59411	101	1575	21	1562	27
10	3.282	0.092	0.2463	0.0048	0.49762	90	1418	25	1572	50

11	3.65	0.17	0.2733	0.0084	0.16242	99	1559	43	1573	97
12	3.67	0.12	0.2757	0.0068	0.24242	100	1570	35	1574	66
13	3.337	0.05	0.2474	0.0035	0.49909	90	1424	18	1581	26
14	3.741	0.054	0.2759	0.0037	0.39994	99	1570	19	1581	30
15	4.118	0.064	0.3031	0.0042	0.42387	108	1706	21	1586	29
16	3.97	0.12	0.2918	0.006	0.21157	102	1651	31	1611	61
17	4.016	0.074	0.2917	0.0045	0.48114	102	1650	22	1620	32
18	3.549	0.042	0.2614	0.0027	0.61837	92	1496	14	1620	18
19	3.685	0.062	0.2678	0.004	0.4479	94	1531	20	1630	33
20	4.245	0.098	0.3069	0.005	0.2862	105	1724	25	1640	46
21	3.92	0.11	0.2801	0.0052	0.12825	97	1590	26	1643	52
22	3.961	0.062	0.2865	0.004	0.55479	98	1625	20	1653	23
23	4.203	0.089	0.2963	0.0043	0.43937	101	1671	21	1656	35
24	3.72	0.11	0.2728	0.0078	0.50939	94	1554	40	1657	57
25	3.95	0.11	0.2813	0.0058	0.30554	96	1596	29	1664	58
26	4.204	0.07	0.2969	0.0036	0.48036	100	1677	18	1669	26
27	3.826	0.071	0.2692	0.0045	0.71832	92	1537	22	1669	22
28	3.827	0.056	0.2702	0.0032	0.55903	91	1541	16	1685	22
29	4.226	0.093	0.3004	0.0055	0.30897	101	1696	27	1685	44
30	4.176	0.069	0.2941	0.0046	0.53598	98	1661	23	1689	28
31	3.932	0.091	0.2821	0.005	0.59295	95	1601	25	1692	33
32	4.279	0.072	0.2979	0.0038	0.64399	99	1680	19	1694	24
33	3.972	0.096	0.2808	0.0053	0.45797	94	1595	27	1697	47
34	4.017	0.053	0.2828	0.0036	0.41333	95	1605	18	1697	27
35	3.847	0.074	0.2758	0.0051	0.5625	92	1572	26	1700	33
36	4.03	0.063	0.2791	0.0037	0.44622	93	1588	18	1707	28
37	4.277	0.076	0.2984	0.0044	0.53153	98	1682	22	1709	30
38	4.279	0.063	0.2995	0.0038	0.45517	99	1688	19	1710	28
39	3.931	0.082	0.2751	0.004	0.38364	92	1570	21	1711	37

40	4.361	0.074	0.3008	0.0051	0.37157	99	1694	25	1714	35
41	4.06	0.084	0.2841	0.0054	0.42891	94	1614	28	1714	34
42	4.306	0.073	0.2968	0.004	0.48557	97	1675	20	1720	28
43	3.947	0.068	0.2733	0.0037	0.45377	91	1558	19	1720	29
44	4.519	0.087	0.3066	0.0058	0.55608	100	1726	29	1728	31
45	4.695	0.061	0.3228	0.0038	0.53126	104	1802	19	1729	21
46	4.278	0.071	0.2938	0.0044	0.41541	96	1661	22	1731	33
47	4.188	0.084	0.2961	0.0055	0.69726	96	1671	27	1735	28
48	4.616	0.081	0.3134	0.0047	0.45301	101	1758	23	1740	31
49	4.403	0.081	0.2995	0.0048	0.62408	97	1688	24	1744	26
50	4.434	0.072	0.3034	0.004	0.37532	98	1711	20	1744	32
51	4.147	0.082	0.2871	0.0052	0.69371	93	1629	26	1747	28
52	4.511	0.058	0.3068	0.004	0.41768	98	1728	20	1755	26
53	4.731	0.096	0.3186	0.0052	0.48824	101	1783	26	1759	34
54	5.099	0.087	0.3436	0.005	0.40881	107	1902	24	1773	29
55	4.228	0.08	0.2865	0.0048	0.28005	91	1622	24	1775	43
56	4.316	0.07	0.2924	0.0047	0.64704	93	1653	24	1776	27
57	4.803	0.072	0.324	0.0044	0.68303	102	1808	21	1777	21
58	4.69	0.076	0.3156	0.004	0.64534	100	1769	19	1777	21
59	4.73	0.15	0.3159	0.0068	0.32242	99	1767	34	1784	62
60	4.463	0.058	0.2942	0.0035	0.4408	93	1662	17	1796	23
61	4.822	0.082	0.3201	0.0046	0.39758	100	1789	23	1797	34
62	4.44	0.11	0.2964	0.008	0.61191	92	1672	40	1820	39
63	4.442	0.064	0.2894	0.0047	0.36189	90	1638	23	1826	34
64	4.593	0.069	0.2969	0.0042	0.41263	91	1675	21	1837	29
65	4.591	0.078	0.2962	0.0043	0.62115	91	1671	21	1846	25
66	5.403	0.095	0.3405	0.0068	0.62486	102	1887	33	1854	27
67	4.664	0.072	0.3009	0.0051	0.65569	91	1694	25	1855	22
68	5.52	0.1	0.3545	0.0056	0.58575	105	1960	26	1866	29

69	5.44	0.11	0.3269	0.0054	0.48688	94	1824	27	1941	33
70	5.254	0.077	0.3163	0.004	0.42949	90	1770	19	1958	27
71	5.47	0.083	0.3279	0.0052	0.65289	92	1827	25	1987	24
72	7.44	0.12	0.3986	0.0056	0.62183	99	2161	26	2172	21
73	6.74	0.13	0.3645	0.0057	0.7204	92	2004	27	2174	20
74	9.44	0.14	0.4598	0.0067	0.60501	104	2437	29	2340	22
75	9.23	0.15	0.4391	0.0067	0.70614	99	2345	30	2379	21
76	8.39	0.11	0.3987	0.0051	0.63704	91	2162	24	2386	20
77	8.51	0.12	0.4002	0.0063	0.58433	90	2168	29	2398	23
78	10.69	0.14	0.5022	0.0068	0.75061	109	2626	29	2407	15
79	9.9	0.13	0.462	0.0056	0.52906	101	2447	25	2415	20
80	10.94	0.17	0.4987	0.0068	0.54258	107	2609	29	2445	23
81	11.75	0.16	0.5086	0.007	0.66138	105	2649	30	2526	18
82	14.18	0.24	0.5349	0.0086	0.53688	99	2760	36	2780	27
83	21.16	0.27	0.63	0.0096	0.67701	100	3146	38	3159	18

J13 - Jamison 1 - MS

	Final 207_235	Final 207_235 _Int2SE	Final 206_238	Final 206_238 _Int2SE	Error Correlation _6_38v7_35	Conc (%)	FinalAge 206_238	FinalAge 206_238 _Int2SE	FinalAge 207_206	FinalAge 207_206 _Int2SE
1	2.916	0.045	0.2379	0.0029	0.40152	98	1375	15	1404	28
2	3.644	0.066	0.2742	0.0047	0.63634	104	1561	24	1502	28
3	3.578	0.065	0.2712	0.0036	0.31818	102	1546	18	1519	35
4	3.566	0.064	0.2707	0.0039	0.56286	102	1543	20	1520	30
5	3.66	0.049	0.2751	0.0032	0.62571	100	1566	16	1562	21
6	3.684	0.066	0.2743	0.0036	0.56979	100	1564	19	1564	26
7	3.311	0.067	0.245	0.0033	0.19052	90	1412	17	1568	40
8	3.453	0.052	0.2551	0.0029	0.46378	93	1464	15	1575	26

9	3.627	0.046	0.2623	0.0029	0.6507	95	1503	15	1576	20
10	3.994	0.056	0.2885	0.004	0.45276	102	1633	20	1596	26
11	4.48	0.13	0.3064	0.0072	0.3019	105	1721	35	1641	57
12	3.961	0.049	0.2778	0.0029	0.59936	96	1581	15	1655	18
13	4.34	0.07	0.2997	0.0042	0.73923	100	1689	21	1690	19
14	3.905	0.069	0.2685	0.0038	0.43495	90	1532	19	1693	29
15	3.991	0.06	0.2738	0.0034	0.49863	92	1560	17	1703	27
16	4	0.053	0.2764	0.0031	0.6748	92	1572	16	1715	18
17	4.03	0.062	0.2753	0.004	0.68106	91	1567	20	1720	21
18	4.681	0.08	0.3144	0.0056	0.78692	102	1762	27	1721	19
19	4.103	0.058	0.2757	0.0032	0.64891	91	1570	16	1721	21
20	4.453	0.054	0.302	0.0029	0.49939	98	1701	14	1728	20
21	4.114	0.064	0.2787	0.0034	0.63202	91	1585	17	1733	22
22	4.8	0.091	0.3194	0.0044	0.50115	103	1786	22	1736	32
23	5.02	0.1	0.334	0.0049	0.71005	107	1857	24	1738	25
24	4.565	0.088	0.3087	0.0048	0.48055	100	1733	24	1738	34
25	4.377	0.083	0.2937	0.0046	0.69007	95	1659	23	1745	25
26	4.736	0.059	0.3208	0.0038	0.60666	103	1793	18	1748	18
27	4.823	0.063	0.3275	0.0031	0.57275	104	1826	15	1749	20
28	4.876	0.06	0.3268	0.0036	0.5779	104	1824	17	1752	19
29	5.012	0.082	0.3391	0.0047	0.462	107	1881	23	1756	30
30	4.418	0.077	0.3	0.004	0.53553	96	1694	20	1757	25
31	4.451	0.062	0.2979	0.0041	0.334	96	1680	20	1758	27
32	4.959	0.078	0.3239	0.0046	0.51429	102	1808	22	1765	27
33	4.8	0.099	0.3175	0.0065	0.71609	101	1777	32	1767	26
34	5.304	0.076	0.353	0.0045	0.40877	110	1948	21	1774	26
35	4.505	0.056	0.2955	0.0035	0.69741	93	1670	18	1793	16
36	4.47	0.06	0.2936	0.004	0.61573	92	1659	20	1798	22
37	4.54	0.1	0.2996	0.0046	0.47851	94	1688	23	1800	38

38	5.133	0.096	0.3318	0.0051	0.70296	102	1848	25	1820	25
39	5.136	0.06	0.3241	0.0033	0.56136	97	1813	16	1865	19
40	5.78	0.067	0.3599	0.0039	0.66382	105	1982	18	1879	16
41	4.94	0.1	0.3169	0.0058	0.62192	94	1773	28	1879	31
42	5.47	0.1	0.3467	0.0045	0.33967	102	1918	22	1886	32
43	9.48	0.14	0.4172	0.0048	0.50228	90	2247	22	2498	21

M8 - McManus 1 - MS

	Final 207_235	Final 207_235 _Int2SE	Final 206_238	Final 206_238 _Int2SE	Error Correlation _6_38v7_35	Conc (%)	FinalAge 206_238	FinalAge 206_238 _Int2SE	FinalAge 207_206	FinalAge 207_206 _Int2SE
1	3.804	0.078	0.2874	0.006	0.42037	106	1631	30	1538	40
2	3.51	0.1	0.2612	0.0068	0.38274	96	1499	34	1569	57
3	3.565	0.079	0.2655	0.0047	0.39203	97	1518	24	1572	41
4	3.47	0.11	0.2525	0.0067	0.056987	91	1449	35	1589	84
5	3.668	0.099	0.2692	0.0064	0.18911	96	1540	33	1597	63
6	3.96	0.16	0.28	0.01	0.67951	96	1589	52	1649	61
7	3.879	0.074	0.2793	0.0038	0.25475	95	1589	20	1667	40
8	4.07	0.1	0.2842	0.006	0.19341	96	1613	30	1686	57
9	4.181	0.095	0.2848	0.0051	0.39113	93	1614	26	1732	43
10	4.671	0.089	0.3139	0.0056	0.41407	101	1758	27	1738	38
11	4.65	0.12	0.312	0.0072	0.39397	100	1747	36	1745	49
12	4.3	0.23	0.278	0.015	0.36681	90	1582	74	1750	120
13	4.36	0.16	0.2883	0.0091	0.33497	93	1629	45	1757	72
14	4.52	0.1	0.3043	0.0056	0.35948	97	1710	28	1763	42
15	4.76	0.1	0.311	0.0067	0.36576	98	1743	33	1775	43
16	4.74	0.13	0.3108	0.0076	0.3777	98	1741	37	1778	54
17	4.429	0.091	0.2923	0.0046	0.46589	93	1652	23	1780	35

18		4.54	0.12	0.2992	0.0055	0.39245	94	1688	28	1788	48
19		4.35	0.31	0.291	0.022	0.26054	91	1650	100	1820	170
20		5.03	0.096	0.3255	0.0053	0.42213	100	1819	26	1821	35
21		8.92	0.16	0.4115	0.0087	0.43208	93	2223	39	2391	35
22		15.16	0.36	0.527	0.011	0.5495	95	2725	44	2871	33

M11 - McManus 1 - MS

	Final 207_235	Final 207_235 _Int2SE	Final 206_238	Final 206_238 _Int2SE	Error Correlation _6_38v7_35	Conc (%)	FinalAge 206_238	FinalAge 206_238 _Int2SE	FinalAge 207_206	FinalAge 207_206 _Int2SE
1	3.476	0.076	0.2615	0.0048	0.35621	98	1496	25	1527	45
2	3.355	0.086	0.2506	0.0054	0.22977	93	1439	28	1550	57
3	3.92	0.12	0.2829	0.0074	0.38548	100	1604	37	1600	61
4	3.68	0.15	0.27	0.011	0.19517	96	1539	57	1610	110
5	3.784	0.099	0.2701	0.0059	0.35128	95	1545	31	1625	54
6	4.02	0.13	0.2887	0.0063	0.26634	101	1636	32	1627	60
7	4.24	0.24	0.283	0.013	0.40937	95	1615	68	1697	97
8	4.61	0.11	0.3116	0.0067	0.27793	101	1752	33	1728	51
9	4.13	0.11	0.2816	0.0063	0.24153	92	1598	32	1733	60
10	4.7	0.12	0.3177	0.0068	0.21079	102	1778	33	1745	55
11	4.24	0.13	0.2851	0.006	0.2833	92	1614	30	1750	56
12	4.21	0.14	0.2831	0.0084	0.52633	91	1604	42	1759	54
13	4.29	0.11	0.2883	0.0056	0.33883	92	1631	28	1777	49
14	4.63	0.16	0.3048	0.0074	0.25567	96	1712	36	1790	74
15	4.72	0.13	0.306	0.0064	0.37811	95	1724	31	1817	48
16	4.9	0.1	0.3172	0.0049	0.47501	97	1774	24	1823	31
17	5.62	0.14	0.3334	0.0055	0.25	94	1855	26	1978	50
18	11.78	0.29	0.463	0.01	0.45116	92	2450	44	2654	42

A3 - Altree 2 - BS

	Final 207_235	Final 207_235 _Int2SE	Final 206_238	Final 206_238 _Int2SE	Error Correlation _6_38v7_35	Conc (%)	FinalAge 206_238	FinalAge 206_238 _Int2SE	FinalAge 207_206	FinalAge 207_206 _Int2SE
1	2.582	0.096	0.2225	0.0057	0.42796	109	1294	30	1183	65
2	2.215	0.075	0.2036	0.0046	0.12146	97	1194	25	1237	76
3	2.353	0.057	0.2118	0.0038	0.16504	95	1238	20	1301	57
4	2.575	0.084	0.2205	0.0049	0.30398	95	1284	26	1351	67
5	2.634	0.084	0.2248	0.0042	0.010232	97	1306	22	1352	64
6	2.55	0.13	0.2197	0.0067	0.29101	92	1279	35	1383	93
7	3.08	0.15	0.267	0.011	0.55087	110	1520	54	1387	89
8	3.057	0.073	0.2262	0.0043	0.082035	95	1313	22	1389	49
9	2.96	0.083	0.2543	0.0054	0.31367	104	1458	28	1397	57
10	3.22	0.14	0.2322	0.0064	0.31793	96	1347	33	1402	73
11	2.612	0.095	0.2291	0.0062	0.26952	94	1326	32	1404	75
12	2.537	0.077	0.2304	0.0048	0.21425	95	1338	25	1407	66
13	2.73	0.08	0.2239	0.0048	0.38461	91	1302	25	1429	58
14	3.012	0.085	0.2582	0.0055	0.13767	103	1478	28	1430	65
15	3.121	0.067	0.2695	0.0046	0.35456	108	1543	24	1435	42
16	3.3	0.084	0.2703	0.0059	0.27438	107	1540	30	1439	56
17	3.48	0.11	0.2787	0.0058	0.20206	109	1583	29	1446	63
18	3.2	0.12	0.2499	0.0063	0.54422	98	1435	32	1470	58
19	3.055	0.099	0.2553	0.0072	0.39679	100	1468	36	1475	62
20	3.185	0.098	0.2353	0.0056	0.23974	92	1360	29	1479	63
21	3.31	0.12	0.2872	0.0067	0.34426	110	1628	34	1484	71
22	3.03	0.12	0.2391	0.008	0.66535	91	1382	42	1516	56
23	3.646	0.084	0.2465	0.0043	0.28336	93	1421	22	1523	45

24	3.359	0.079	0.245	0.0044	0.33955	92	1413	23	1534	43
25	3.897	0.078	0.2915	0.0047	0.37438	107	1650	23	1539	40
26	3.41	0.14	0.256	0.0093	0.61239	94	1475	50	1577	71
27	3.82	0.14	0.2546	0.0064	0.34891	91	1460	33	1609	72
28	3.35	0.08	0.2576	0.0055	0.38493	91	1476	28	1626	47
29	3.98	0.21	0.3237	0.0076	0.44674	110	1804	37	1641	81
30	4.144	0.092	0.2911	0.0056	0.37024	98	1647	28	1685	43
31	4.21	0.11	0.2822	0.0054	0.19593	94	1600	27	1696	55
32	5.13	0.11	0.3056	0.0057	0.20293	94	1717	28	1835	48
33	16.37	0.26	0.5865	0.0098	0.57952	103	2971	40	2880	25

A1 - Altree 2 - JS

	Final 207_235	Final 207_235 _Int2SE	Final 206_238	Final 206_238 _Int2SE	Error Correlation _6_38v7_35	Conc (%)	FinalAge 206_238	FinalAge 206_238 _Int2SE	FinalAge 207_206	FinalAge 207_206 _Int2SE
1	1.938	0.055	0.1803	0.0034	0.24484	98	1068	19	1092	55
2	2.047	0.063	0.1942	0.0039	0.031245	105	1143	21	1093	75
3	2.012	0.079	0.1919	0.0044	0.2934	103	1131	24	1095	77
4	2.03	0.061	0.1849	0.0041	0.15094	97	1095	22	1124	74
5	2.082	0.06	0.1972	0.0036	0.081891	103	1161	20	1126	66
6	2.032	0.067	0.1893	0.0036	0.24524	99	1117	20	1126	66
7	2.28	0.19	0.202	0.012	0.040596	105	1185	64	1130	230
8	2.096	0.077	0.1962	0.0045	0.11759	102	1154	24	1132	78
9	2.42	0.11	0.2123	0.0094	0.22248	91	1249	47	1370	150
10	3.18	0.15	0.2652	0.0091	0.38894	105	1514	46	1438	97
11	2.86	0.11	0.2239	0.0064	0.013103	90	1301	34	1439	92
12	3.53	0.12	0.2713	0.0055	0.026843	106	1553	27	1472	76
13	3.53	0.12	0.2746	0.0056	0.2222	106	1562	28	1476	64

14	3.16	0.1	0.2424	0.0055	0.19108	95	1402	29	1481	68
15	3.25	0.1	0.2521	0.0056	0.29407	98	1451	29	1484	61
16	3.045	0.06	0.2348	0.0036	0.5493	92	1360	19	1484	33
17	3.469	0.095	0.2753	0.0052	0.23445	105	1565	26	1492	55
18	3.449	0.095	0.2627	0.0054	0.31704	100	1502	27	1497	58
19	3.24	0.11	0.2552	0.0068	0.48907	98	1463	35	1498	67
20	2.82	0.27	0.244	0.014	0.081834	94	1408	75	1500	200
21	3.559	0.078	0.2721	0.0041	0.27357	103	1550	21	1505	46
22	3.399	0.073	0.2566	0.004	0.33521	98	1471	21	1508	40
23	3.305	0.081	0.2583	0.0054	0.28667	98	1483	28	1514	52
24	3.482	0.091	0.2692	0.0054	0.074415	101	1537	27	1515	59
25	3.524	0.075	0.2664	0.0041	0.2615	100	1523	21	1524	41
26	3.274	0.09	0.2457	0.0053	0.35719	92	1414	27	1529	57
27	3.88	0.078	0.2907	0.0044	0.37469	106	1644	22	1546	38
28	3.46	0.31	0.264	0.016	0.73679	97	1506	79	1550	120
29	3.49	0.11	0.2603	0.0066	0.33264	96	1490	34	1552	65
30	3.23	0.1	0.2431	0.0053	0.29094	91	1408	26	1552	62
31	3.676	0.074	0.2832	0.0054	0.21221	103	1606	27	1561	45
32	3.239	0.097	0.2454	0.005	0.51664	90	1414	26	1569	49
33	3.72	0.25	0.271	0.01	0.31488	99	1549	54	1570	120
34	3.594	0.093	0.2683	0.005	0.26418	97	1530	25	1583	51
35	3.696	0.096	0.2797	0.0046	0.20278	100	1591	24	1587	51
36	3.506	0.091	0.2656	0.005	0.25131	96	1517	25	1588	50
37	3.65	0.13	0.2673	0.0065	0.16802	96	1531	33	1589	76
38	3.77	0.12	0.2808	0.0066	0.40136	100	1593	33	1591	56
39	3.69	0.16	0.27	0.0067	0.25625	97	1542	34	1591	77
40	3.522	0.092	0.2685	0.0045	0.2437	96	1532	23	1592	49
41	3.9	0.18	0.267	0.01	0.23149	95	1523	51	1599	94
42	3.967	0.077	0.2866	0.0037	0.18674	100	1623	19	1618	37

43	3.973	0.069	0.2779	0.0044	0.36749	96	1580	22	1654	33
44	3.65	0.21	0.263	0.012	0.30643	91	1506	58	1660	120
45	4.017	0.084	0.2761	0.0049	0.50087	92	1570	25	1698	36
46	6.35	0.13	0.353	0.0065	0.49383	93	1947	31	2092	32
47	8.92	0.31	0.439	0.012	0.32353	98	2344	53	2402	55

A2 - Altree 2 - JS

	Final 207_235	Final 207_235 _Int2SE	Final 206_238	Final 206_238 _Int2SE	Error Correlation _6_38v7_35	Conc (%)	FinalAge 206_238	FinalAge 206_238 _Int2SE	FinalAge 207_206	FinalAge 207_206 _Int2SE
1	1.856	0.055	0.1605	0.0033	0.30086	97	959	18	987	68
2	1.909	0.055	0.1672	0.004	0.31935	98	995	22	1014	65
3	2.011	0.073	0.1719	0.0043	0.17299	98	1021	23	1042	85
4	1.809	0.055	0.1863	0.0041	0.1861	105	1100	22	1045	67
5	1.9	0.1	0.1718	0.0054	0.14958	95	1019	29	1070	120
6	2.07	0.14	0.1875	0.0076	0.21802	101	1106	41	1100	150
7	1.822	0.06	0.1775	0.0057	0.41272	95	1052	31	1106	71
8	2.114	0.079	0.2023	0.0056	0.14216	107	1185	30	1109	86
9	2.05	0.11	0.1904	0.006	0.042054	99	1121	32	1130	130
10	2.222	0.069	0.2036	0.0041	0.2912	105	1195	21	1140	66
11	2.184	0.051	0.2012	0.0035	0.091237	103	1180	19	1145	57
12	2.185	0.082	0.2002	0.0049	0.26058	103	1179	26	1145	79
13	2.17	0.1	0.1911	0.0043	0.076422	97	1126	23	1163	95
14	2.234	0.062	0.2062	0.0039	0.03851	103	1207	21	1169	67
15	2.1	0.13	0.1919	0.0086	0.11668	96	1129	46	1170	150
16	2.002	0.088	0.1855	0.0047	0.34768	93	1096	26	1173	79
17	2.098	0.077	0.1912	0.0044	0.31608	94	1128	24	1205	76
18	2.306	0.089	0.2074	0.0051	0.39365	97	1214	27	1248	70

19	2.653	0.079	0.2308	0.0048	0.2986	101	1337	25	1323	55
20	2.842	0.088	0.2409	0.0051	0.19461	103	1393	26	1357	66
21	3.083	0.066	0.2284	0.004	0.52971	98	1329	21	1359	37
22	3.045	0.074	0.2588	0.0049	0.49307	108	1485	25	1371	41
23	2.595	0.069	0.2221	0.005	0.29857	94	1297	26	1385	60
24	2.87	0.076	0.2361	0.0042	0.23893	98	1365	22	1396	52
25	3.08	0.11	0.2246	0.0077	0.62312	93	1304	40	1396	57
26	3.327	0.077	0.2468	0.0061	0.56218	98	1423	31	1445	45
27	3.26	0.21	0.2508	0.0097	0.091373	99	1446	48	1460	120
28	3.107	0.079	0.2404	0.0043	0.1552	95	1389	22	1463	54
29	3.47	0.075	0.2738	0.0051	0.28334	106	1558	26	1475	49
30	3.568	0.097	0.2745	0.0054	0.3501	105	1561	27	1489	53
31	3.129	0.06	0.2333	0.0042	0.21566	91	1351	22	1492	46
32	3.05	0.15	0.245	0.011	0.62018	94	1408	57	1502	82
33	3.73	0.11	0.2877	0.0064	0.15888	108	1630	31	1508	63
34	3.38	0.1	0.2597	0.0061	0.34565	98	1486	31	1511	58
35	3.55	0.079	0.2667	0.0052	0.35657	100	1524	27	1524	45
36	3.331	0.082	0.2503	0.0047	0.25032	95	1443	24	1525	50
37	3.66	0.13	0.2762	0.0063	0.29907	103	1569	32	1530	68
38	3.632	0.098	0.2779	0.0056	0.31964	103	1579	28	1534	49
39	3.73	0.1	0.2808	0.0054	0.21493	104	1596	28	1535	55
40	3.22	0.14	0.2476	0.0078	0.15242	93	1425	40	1535	90
41	3.76	0.11	0.2775	0.0063	0.19632	103	1579	32	1537	65
42	3.527	0.088	0.2678	0.0049	0.070715	99	1528	25	1538	55
43	3.556	0.08	0.2645	0.004	0.32747	98	1511	20	1542	44
44	3.4	0.12	0.2568	0.0062	0.27074	96	1476	32	1543	68
45	3.92	0.15	0.28	0.0096	0.54368	103	1589	48	1546	63
46	3.73	0.12	0.2775	0.0073	0.10805	102	1578	36	1550	77
47	3.95	0.13	0.2922	0.0072	0.19157	107	1659	35	1554	71

48	3.58	0.11	0.2711	0.0065	0.29358	99	1543	33	1558	66
49	3.246	0.078	0.2445	0.0055	0.18306	91	1411	29	1559	56
50	3.37	0.15	0.247	0.01	0.52336	91	1420	52	1566	76
51	3.89	0.15	0.288	0.01	0.31029	104	1633	52	1569	86
52	3.68	0.14	0.2659	0.0068	0.032041	96	1519	35	1576	82
53	3.72	0.12	0.2792	0.0055	0.22494	101	1585	28	1577	61
54	3.724	0.094	0.2759	0.0056	0.30709	99	1568	29	1585	52
55	3.71	0.11	0.2689	0.0057	0.22732	97	1533	29	1587	62
56	3.83	0.11	0.2795	0.0063	0.24371	100	1586	32	1591	60
57	3.58	0.11	0.2621	0.0059	0.22301	94	1498	30	1593	57
58	3.45	0.11	0.2482	0.0046	0.16135	90	1432	24	1593	58
59	3.861	0.077	0.28	0.0051	0.34928	100	1590	26	1597	44
60	3.78	0.12	0.2759	0.0054	0.28946	98	1573	28	1599	61
61	3.845	0.099	0.278	0.0055	0.36886	99	1579	28	1600	50
62	3.91	0.11	0.284	0.0048	0.20075	100	1614	24	1619	56
63	3.84	0.24	0.283	0.012	0.10157	99	1608	63	1620	140
64	3.85	0.14	0.2761	0.0073	0.19682	96	1568	37	1627	82
65	4.28	0.32	0.302	0.017	0.12248	103	1697	82	1650	170
66	4	0.21	0.2842	0.0089	0.052331	98	1610	45	1650	110
67	3.82	0.1	0.2652	0.0055	0.32106	91	1514	28	1659	50
68	3.98	0.15	0.2753	0.0068	0.13301	93	1564	34	1680	72
69	3.9	0.12	0.265	0.0055	0.28112	90	1516	28	1693	60
70	4.63	0.13	0.3123	0.0071	0.30256	100	1748	35	1742	55
71	4.831	0.096	0.3235	0.0056	0.28641	103	1808	28	1756	44
72	4.91	0.1	0.3243	0.0066	0.42247	100	1811	33	1814	38
73	10.03	0.19	0.4509	0.0081	0.4908	98	2395	36	2455	32

APPENDIX C: PROVENANCE TERRANES DATA

Table 4: Potential provenance terranes, peak data from kernel density plot Fig. 13

Provenance terrane	PCO	HCO	ARN	G&C	ISA	ARU	MUS	MO	YA	MA
Age population peaks (Ma)	**1860**	**1860**	1710	**1580**	1580	1560	**1190**	1230	**1775**	**1650**
	2025	2550	**1840**	1640	1670	1630	1590	**1695**		
	2525			1810	**1740**	1685	1695	1765		
					1780	**1770**	1745			
					1860	**1800**				

PCO = Pine Creek Province, HCO = Halls Creek Province, ARN = Arnhem Province, G&C = Georgetown and Coen Region, ISA = Mount Isa Province, ARU = Arunta Region, MUS = Musgrave Province, MO = Mojave Province, YA = Yavapai Province, MA = Mazatzal Province. Dominant peak in bold, second dominant peak underlined.

APPENDIX D: ANALYTICAL METHODOLOGY – EXTENDED

Separation of zircon from host rock

Zircons were separated from host sandstones via crushing and milling (3 times), the disaggregated material was sieved to separate out the potential zircon component (>79µm to <400µm). The zircon component was panned to remove light mineral fractions and concentrate the heavy mineral fraction, which was dried and magnetic minerals were remove via a rare earth magnet, (Frantz machine was broken), zircon are non magnetic, therefore were not removed.
The zircon component was processed through high density liquid (lithium heteropolytungstates) to further remove light mineral fractions of density less than 2.8g/cm^3 (for example quartz and feldspar will float), the denser component sinks and was frozen with dry ice (frozen CO_2) to be easily separated from the lighter component which was removed. The denser zircon rich component was washed to remove heavy liquid with deionised water and dried.

Picking zircon

Zircon rich sample was poured in to glass dish, zircons were identified under binocular microscope and 'picked' by hand using a fine tipped pick. Picked zircons were stuck to the base of a mount and held in place by double sized tap. This process of mounting zircons was repeated until a sufficient number of zircons were acquired, (~100 or all visible zircons in the sample).

Epoxy resin zircon mounts

The base of the mount was coupled with the circular enclosing form of the mount (coated with Vaseline to allow for easy removal after mount has set). Epoxy resin was prepared using a two part epoxy resin, one part epoxy (5g), one part harder (1.2g). These two parts were mixed for 2-3 minutes, then heated for 2 minutes at 50^{o}C. The heated mixed resin was slowly poured into the zircon mount, then covered and left for 24 hours to set. The Vaseline was cleaned off the zircon mount using ethanol. This process used for all mounts.

Polish zircon mounts

Step 1:
The zircon mounts were polished to remove some of the epoxy resin to semi expose the zircons. 2000µm grit sandpaper was wet with water prior to rubbing/sanding the base of the mounts. The mounts were rubbed with a figure eight motion and turned (rotated by a third of a revolution) every 20 seconds, the mounts were checked every minute under a binocular microscope to examine the progress of exposing mounted zircons.
Step 2:
1000µm grit sandpaper was wet with water, then the mounts were polished with the same figure eight motion, and checked every minute under a binocular microscope to monitor the progress of the mounts.
Step 3:
Mounts were polished with 3µm grit sandpaper for 10 minutes with constant rotation.
Step 4:
Mounts were polished with 1µm grit sandpaper for 10 minutes with constant rotation.
Step 5:
Mounts were cleaned in a sonic water bath for 10 minutes.

Carbon coated zircon mounts

Mounts required carbon coating, prior to imaging by scanning electron microscope (SEM). The base of mounts required a carbon coating over zircons to reduce the resistivity to allow quality.

CL-SEM – Adelaide Microscopy

Mounts were imaged using SEM, move specifically by cathodoluminescence (CL) imaging, to map zircon mounts at Adelaide Microscopy (address: Ground Floor NG13, Medical School North Frome Road The University of Adelaide SA 5005), using a 15mm working distance between mount surface and probe, CL operated at 15kV, with a pot size of 7µm, under high vacuum conditions. CL images were used to determine zircon structure, so the core can be targeted.

U-Pb detrital zircon geochronology: LA-ICP-MS

U-Pb zircon analysis for mounts, were undertaken at Adelaide Microscopy (same location). Analysis of detrital zircon obtained U-Pb ages using laser ablation ICP-MS with cation analysis, UP-213NdYag New Wave pulsed solid state laser coupled with Agilent 7500cx ICP- Quadrupole Mass Spectrometer and the method described by Payne et al. (2010).
LA-ICP-MS setup for all data; acquired with single spot analysis on individual zircon grain with a beam spot size diameter of 30µm, frequency of 5 Hz, laser intensity was set to 70% (~5 to 7 J/cm^2), targeting mainly zircon cores and some outside of rims, background record for 30 seconds, ablation recorded for 30 seconds, after ablation 30 seconds of flushing not recorded.
Run sequence order: 8 GJ-1 spots (at the beginning of each run, then reduced to 5 thereafter), 3 PLESOVICE spots, 2 GJ-1 spots, 15 zircon spots (from zircon mount), 5 GJ-1 spots, 3 PLESOVICE spots, 2 GJ-1 spots. Sequence repeated to a maximum of 288 spots per run.
U-Pb data corrected in Iolite (Chew et al., 2013) via standard GJ-1; known TIMS age $^{206}Pb/^{238}U$ = 600.7 ± 1.1 Ma and $^{207}Pb/^{235}U$ = 602.2 ± 1.0 Ma (Jackson et al., 2004), PLESOVICE standard; known TIMS age $^{206}Pb/^{238}U$ = 337.13 ± 0.37 Ma and $^{207}Pb/^{235}U$ = 337.27 ± 0.11 Ma (Slama et al., 2008) was used to check the accuracy of GJ-1 corrected output data, both GJ-1 and PLESOVICE error are 2 standard deviations.
All Beetaloo Basin sampled U-Pb data found in Table 3, Appendix B.

Concordia plots were created using Isoplot 3.00 in Excel (Ludwig, 2003).
Multidimensional Scaling (MDS) plots and multi kernel distributions were created using R software package (Vermeesch, 2013).
Ages of single analyses are quoted at 2 sigma level, the maximum deposition age is calculated from the youngest >95% concordant analysis within analytical uncertainty (Spencer et al., 2016). All zircon U-Pb near-concordant (90-110%) data found in Table 3, Appendix B. Many data yielded Mesoproterozoic ages that are at part of geological time where $^{206}Pb/^{238}U$ ages become more precise than $^{207}Pb/^{206}Pb$ ages due to the differing half lives of U^{238} and U^{235}. I have followed Nemchin and Cawood (2005) here in quoting the age with the lowest error as the best estimate of the grains age.